

# Perfect Counterfactuals in Imperfect Worlds: Modelling Noisy Implementation of Actions in Sequential Algorithmic Recourse

Yueqing Xuan<sup>1\*</sup>, Kacper Sokol<sup>2</sup>, Mark Sanderson<sup>1</sup>, Jeffrey Chan<sup>1</sup>

<sup>1</sup>ARC Centre of Excellence for Automated Decision-Making and Society,  
School of Computing Technologies, RMIT University, Australia.

<sup>2</sup>Department of Computer Science, ETH Zurich, Switzerland.

\*Corresponding author(s). E-mail(s): [yueqing.xuan@student.rmit.edu.au](mailto:yueqing.xuan@student.rmit.edu.au);

Contributing authors: [kacper.sokol@inf.ethz.ch](mailto:kacper.sokol@inf.ethz.ch);  
[mark.sanderson@rmit.edu.au](mailto:mark.sanderson@rmit.edu.au); [jeffrey.chan@rmit.edu.au](mailto:jeffrey.chan@rmit.edu.au);

## Abstract

Algorithmic recourse provides actions to individuals who have been adversely affected by automated decision-making and helps them achieve a desired outcome. Knowing the recourse, however, does not guarantee that users would implement it perfectly, either due to environmental variability or personal choices. Recourse generation should thus anticipate its sub-optimal or noisy implementation. While several approaches have constructed recourse that accounts for robustness to small perturbation (i.e., noisy recourse implementation), they assume an entire recourse to be implemented in a single step and thus apply one-off uniform noise to it. Such assumption is unrealistic since recourse often includes multiple sequential steps which becomes harder to implement and subject to more noise. In this work, we consider recourse under plausible noise that adapts to the local data geometry and accumulates at every step of the way. We frame this problem as a Markov Decision Process and demonstrate that the distribution of our plausible noise satisfies the Markov property. We then propose the ROBust SEquential (ROSE) recourse generator to output a sequence of steps that will lead to the desired outcome even under imperfect implementation. Given our plausible modelling of sub-optimal human actions and greater recourse robustness to accumulated uncertainty, ROSE can grant users higher chances of success under low recourse costs. Empirical evaluation shows our algorithm manages the inherent trade-off between recourse robustness and costs more effectively while ensuring its low sparsity and fast computation.

**Keywords:** Counterfactual explanation, Robustness, Markov decision process, Plausibility, Algorithmic recourse, Sequential recourse.

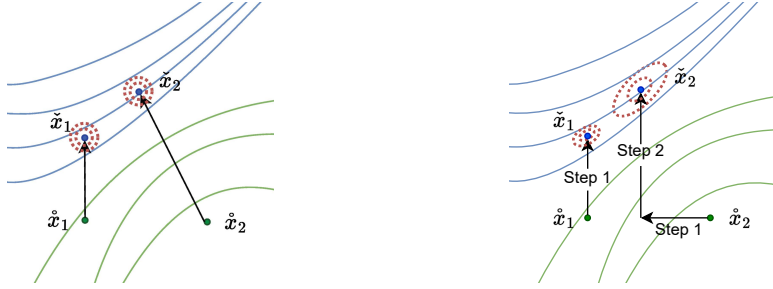
## 1 Introduction

Automated decision-making has become ubiquitous in high-stakes domains such as finance and healthcare. This creates a need to empower affected individuals by offering them counterfactual explanations (CEs), i.e., algorithmic recourse, to help them achieve the desired outcome [Wachter et al., 2017]. Prior work on CEs suggests to explainees what features to alter, and by how much, to change the model’s prediction [Ustun et al., 2019; Joshi et al., 2019]. For example, when a person’s loan application is denied by a model employed by a bank, they should be provided with a CE that informs them to increase their income by \$1,000 and reduce their consumer debt by \$5,000 to have the loan application accepted.

However, simply highlighting feature-wise differences between factual and counterfactual instances suggests that these changes can be achieved instantly and simultaneously in a one-shot step [Verma et al., 2020]. In practice, users will not necessarily be able to make all of the suggested changes suddenly; instead they may need to make incremental changes through a sequence of discrete actions [Barocas et al., 2020]. In the previous example, a realistic guidance to a user might be to reduce debt first and then increase income. This is known as (prospective) sequential recourse that generates a sequence of discrete actions leading to a counterfactual outcome [Ramakrishnan et al., 2020; Kanamori et al., 2021; Verma et al., 2022].

Current methods generate counterfactuals under the assumption that users will implement them faithfully; however, in the real world, recourse is often subject to noisy implementation [Pawelczyk et al., 2023]. Prior research has noted that recourse involving multiple actions is often noisily implemented [Björkegren et al., 2020], and that humans tend to follow sequential instructions imperfectly [DeGrandpre and Buskist, 1991]. To complicate matters further, individuals might lack precise control over the value of a feature when taking an action [Barocas et al., 2020], or feature values might be unintentionally changed due to unforeseen circumstances [Virgolin and Fracaros, 2023]. Consequently, uncertainty could arise while executing actions, causing feature values to diverge from what a user is expecting after a discrete step. For example, a user who planned to increase their income by \$1,000 may eventually end up with a factual raise of \$990 due to inflation. In this case, users should ideally still end up in the desirable position once they have completed the original recourse, i.e., counterfactual generation methods should be robust to users’ genuine but possibly sub-optimal behaviours.

Current literature also agrees that a longer recourse is harder to implement as it often entails more actions or the scale of each action is larger, which increases the complexity of its implementation. Intuitively, users are less likely to faithfully follow the recourse as the process gets longer, thus uncertainty in human actions – i.e., noise – can accumulate along the recourse-seeking process. However, existing recourse generators assume that simple recourse is equally uncertain as complex recourse and robustify the



(a) Same scale of Gaussian noise added to the recourse of varying length. (b) Larger plausible noise that adapts to the local data geometry added to longer recourse.

**Fig. 1:** Examples of the robust recourse by existing method and our framework. The blue lines enclose the desirable region. The contours indicate data density. Panel (a) shows that prior work [Pawelczyk et al., 2023; Guyomard et al., 2023] applies the same size of noise to recourse of varying length; plausibility of noise is also ignored. In Panel (b), we consider that longer recourse is vulnerable to larger uncertainty and we model plausible noise that follows the local data geometry.

former against unnecessarily large noise, penalising its distance. On the other hand, complex recourse is only robust to smaller uncertainty, so users are still likely to fail (see Figure 1a). To this end, we address robust recourse in a more realistic setting where each recourse consists of multiple discrete actions of varied size, and uncertainty is associated with each action thus accumulates as the process gets longer (see Figure 1b). Since the magnitude of noise we model is adaptive to the recourse distance, shorter recourse will not be penalised by additional costs to address unrealistically large uncertainty whereas longer recourse is granted with greater robustness.

When infusing recourse with noise to model noisy recourse implementation in the real-world setting, the distribution of noise should be realistic and evidenced by sufficient data. To this end, we introduce plausible noise distribution and demonstrate the Markov property of plausible noise associated with steps in recourse. We further model the robust recourse generation problem as a Markov Decision Process (MDP). Our work is complementary to the work [Pawelczyk et al., 2023] and [Guyomard et al., 2023], which ignore plausibility or increasing uncertainty when modelling noisy implementation, and to the work [Dominguez-Olmedo et al., 2022], which models causal noise under the explicit knowledge of causal models. Our noise formulation can be easily generalised without the knowledge of causal models and simultaneously captures plausibility.

Our contribution is threefold. (1) In Section 3.2 we model plausible noise to represent noisy implementation of human actions. (2) Section 3.3 formulates the distribution of accumulated plausible noise and shows its Markov property. Then we use an MDP to model the accumulation of plausible noise along the recourse-seeking process. (3) In Section 4 we propose the ROBust SEquential (ROSE) recourse generator that offers users sequential recourse robust to noisy implementation. As a result, our robust recourse is more realistic than instantaneous counterfactuals, and grants users higher

chances of success even if they cannot implement every action precisely. Our plausible modelling of sub-optimal human actions allows robust recourse to stay low costs. An extensive evaluation with three real-world datasets and seven baselines demonstrates our superior performance in robustness and feature sparsity while effectively managing the trade-off between robustness and recourse costs.

## 2 Related Work

### 2.1 Sequential Counterfactual Explanations:

Existing CE methods suggest changes to feature values that lead to a desired outcome. Common objectives considered include proximity between factual and counterfactual instances [Russell, 2019; Ustun et al., 2019; Karimi et al., 2020], number of changed features (sparsity) [Van Looveren and Klaise, 2021; Mothilal et al., 2020; Dandl et al., 2020], and feasibility of counterfactual instances through data density or closeness to existing instances [Pawelczyk et al., 2020a; Downs et al., 2020; Joshi et al., 2019; Van Looveren and Klaise, 2021]. However, these methods only return the counterfactual instances, which reflects their assumption that recourse is an instantaneous, one-step process [Verma et al., 2020]. In reality, changes do not happen instantly but through a sequence of discrete steps [Verma et al., 2020; Naumann and Ntoutsis, 2021]. Recent papers have proposed sequential counterfactual generation. E.g., FACE provides a sequence of existing data instances as a path to the target counterfactual [Poyiadzi et al., 2020], and different optimisation techniques, such as MDP, exist [Ramakrishnan et al., 2020; Kanamori et al., 2021; Naumann and Ntoutsis, 2021; Verma et al., 2022]. Despite recent interest in producing sequential actions to support recourse, little attention has been paid to the possibility of its noisy implementation, which may easily invalidate recourse.

The aforementioned work that produces instantaneous counterfactuals is commonly based on supervised learning. Reinforcement learning has recently gained popularity in CE generation where sequential recourse is an integral part. E.g., [Tsirtsis et al., 2021; Tsirtsis and Rodriguez, 2024] focus on time series data and explore “if some historical actions had changed, how the current situation would have been like”. In other words, they address retrospective CEs in sequential settings. However, our work focuses on prospective CEs which inform users what to do in the next steps to get a better outcome in the future. To the best of our knowledge, our paper is the first to model sequential CEs retrospectively under serial uncertainty.

### 2.2 Robustness of Counterfactual Explanations:

Current literature recognises various events to which CEs should be robust. Examples include robustness to shifts of prediction models [Upadhyay et al., 2021], data distribution shifts [Rawal et al., 2020], model multiplicity [Pawelczyk et al., 2020b; Jiang et al., 2024] and (gradual) model re-training [Ferrario and Loi, 2022]. In addition, Sharma et al. [2022] explore whether CE generators give consistent outputs when users check for updated CEs along their original recourse. Raman et al. [2023] define robustness

as CEs residing in dense data regions, but their definition is commonly referred to as *plausibility*.

Our work is closely related to another notion of robustness which deals with the perturbation of feature values. Such perturbation applied to the explained instance has been shown to manipulate or invalidate the corresponding CEs [Slack et al., 2021; Pawelczyk et al., 2023]. In this space, Dominguez-Olmedo et al. [2022] propose a method to robustify counterfactuals against (causal) uncertainty in feature input; Pawelczyk et al. [2023] and Guyomard et al. [2023] propose to handle perturbations applied to the counterfactual instance, which simulates noisy implementation of recourse; Virgolin and Fracaros [2023] study robustness to perturbations of features that are altered and kept unchanged in the recourse. However, these methods assume that the implementation of counterfactuals is a one-shot process, thus they only add a constant amount of noise once to every counterfactual despite their differences in cost and sparsity. This indicates that easier recourse is robustified against unnecessarily large perturbations whereas complex recourse becomes invalidated when uncertainty accumulates. With recent work paying more attention to providing recourse as a sequence of actions, it is important to address the robustness of *sequential* recourse to *accumulated* noise.

In addition, literature on robust counterfactuals has inconsistent formulations of adversarial perturbations to individual data instances. Pawelczyk et al. [2020b] and Guyomard et al. [2023] draw noise once per instance from a Gaussian probability distribution. However, they assume the same magnitude of uncertainty in different recourse regardless of how difficult it is to complete. Dominguez-Olmedo et al. [2022] take into account the linear causal relationships between features by leveraging the explicit knowledge of causal models; however the occurrence of noisy instances from a perturbation set is treated as equally possible. Virgolin and Fracaros [2023] manually define the perturbation ranges for each feature based on domain knowledge, and the perturbation set contains all possible combinations of perturbed feature values. Similarly, they assume the perturbation points within the set are equally likely to occur. Our work incorporates plausibility and accumulated uncertainty into noise formulation which models human’s sub-optimal recourse implementation more realistically. This does not rely on explicit knowledge of causal models or domain information, thus has greater generalisability.

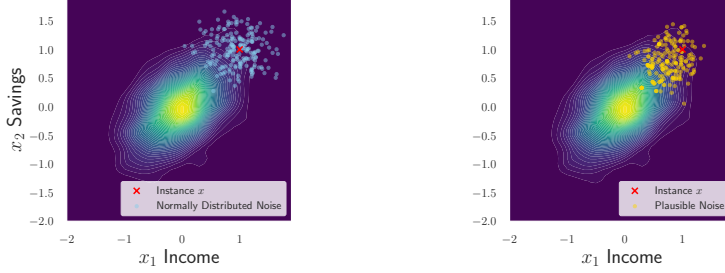
### 3 Noisy Recourse Implementation

In this section, we first define the generic formulation of recourse and MDPs. We then propose novel ways to generate one-off and accumulated plausible noise to capture imperfect recourse implementation.

#### 3.1 General Formulation

***Notation***

Let  $f : \mathcal{X} \rightarrow \mathcal{Y}$  denote a classifier which maps features  $x \in \mathcal{X} \subseteq \mathbb{R}^d$  to labels  $\mathcal{Y}$ . Let  $\mathcal{Y} = \{0, 1\}$  where 0 and 1 denote an unfavourable outcome (e.g., loan denied) and a favourable outcome (e.g., loan approved), respectively. Let  $\hat{x} \in \mathcal{X}$  denote the factual



(a) Normally distributed noise.

(b) Plausible noise.

**Fig. 2:** Two approaches to sample random noise around an instance  $x$  (marked by a red cross). This synthetic toy dataset has two positively-correlated features. The contours indicate the density of the data distribution estimated via kernel density estimation. Current literature assumes (a) normally distributed noise around the selected point, but this distribution fails to account for plausibility. For example, instances with higher income and savings than the chosen point are less plausible despite being close, i.e., there is insufficient data support. Our approach models (b) plausible noise by considering both its distance to the selected point and local data distribution.

instance who seeks recourse, i.e.,  $f(\hat{x}) = 0$ . We denote  $h : \mathcal{X} \rightarrow \mathcal{X}$  a recourse generator that returns a counterfactual instance  $\tilde{x}$  such that  $f(\tilde{x}) = 1$ . Using a pre-defined distance function  $d : \mathbb{R} \rightarrow \mathbb{R}_+$ , we consider  $\delta = d(\hat{x}, \tilde{x})$  to be the recourse distance.

### Markov Decision Process

In this paper, we frame the recourse-finding problem as an MDP (justification for using an MDP is discussed in Section 3.3). In an MDP problem, a user that acts towards recourse is called an *agent* who corresponds to a  $d$ -dimensional data point  $x$ . The combinations of possible values for all features in  $\mathcal{X}$  form the *state space*  $\mathbf{S}$  for the MDP. Upon taking a specific action  $a$ , an agent can move from one state  $s$  to the other state  $s'$ . These actions constitute the *action space*  $\mathbf{A}$  for the MDP. The third component of the MDP is the *transition function* which is represented by  $\mathbf{T} : s \times a \rightarrow s'$ . The final component of the MDP is the *reward function*. It associates each action with a reward where reaching desirable states generates a positive reward.

### Translating CEs to MDPs

When modelling the CE generation for a user through MDP, we assume that the user (agent) starts from the initial state  $s_0 \equiv \hat{x}$ , and takes a sequence of  $k$  (ordered) actions  $\mathcal{A} = \{a_1, \dots, a_k \mid s_{i-1} \times a_i \rightarrow s_i\}$  to get to the counterfactual state  $s_k \equiv \tilde{x}$ . Our goal is finding a policy  $\pi : \mathbf{S} \rightarrow \mathcal{A}$  that, given a starting state  $s_0 \in \mathbf{S}$  (a factual data point), returns the best sequence of actions  $\mathcal{A}$  to take to reach a counterfactual state. In section 4, we will detail the formulation of each component in the MDP to generate robust recourse.

## 3.2 Plausible Noise

Current literature on robust recourse often models perturbations by adding small normally distributed noise  $\epsilon \sim \mathcal{N}(\mathbf{0}, \sigma^2 \cdot \mathbf{I})$  to the counterfactual instance  $\tilde{x}$ . This implies that instances proximate to  $\tilde{x}$  are also expected to be in the desirable class. Given that recourse takes place in the real world, points representing the noisy human implementation of  $\tilde{x}$  should also be realistic in the sense that they lie within the data manifold and follow plausible data distribution. Consider examples in Fig. 2; savings and income are positively correlated. Given the data geometry, we expect noisy instances around  $x$  with both higher income and higher savings to be less likely than those with lower income and lower savings because the former situation lacks sufficient data support. Thus the plausible noise distribution in Fig. 2b is more informative and better reflects realistic human implementation of recourse. Definition 1 formalises our notion of plausible noise.

**Definition 1** (Plausible Noise). *The plausible noise surrounding an instance  $x$  can be modelled by some noise  $\epsilon$  characterised by the probability distribution  $p_x$  where*

$$\epsilon = x' - x \quad \text{s.t.} \quad x' \sim p_x = c \cdot \mathcal{N}(x, \sigma^2 \cdot \mathbf{I}) \cdot K(\mathcal{X}) . \quad (1)$$

$\mathcal{N}(x, \sigma^2 \cdot \mathbf{I})$  is the Gaussian probability distribution with mean vector  $x$  and co-variance matrix  $\sigma^2 \cdot \mathbf{I}$ ;  $K$  is an estimate of a probability density function based on  $\mathcal{X}$ , which reflects the density of underlying data distribution; and  $c$  is the normalisation constant to ensure  $p_x(x')$  integrates to 1.

Intuitively, a small perturbation  $\epsilon$  to  $x$  results in plausibly similar instances  $x'$  around  $x$ . Specifically, the closer a random sample  $x'$  is to  $x$ , and the more likely it obeys the local data geometry around  $x$ , the more likely it is to be drawn. Unlike normally distributed noise [Pawelczyk et al., 2023], our formulation captures noise under a more realistic setting. While noise modelled by a linear Structural Causal Model (SCM) may better account for plausibility [Dominguez-Olmedo et al., 2022], knowing the exact SCM is often infeasible [Verma et al., 2022]; similarly, defining uncertainty range manually for every feature based on domain knowledge is impractical [Virgolin and Fracaros, 2023]. Therefore our noise formulation can operate in a more general setting where the underlying causal model is unknown.

### 3.2.1 Evaluating Plausible Noise

When evaluating the robustness of recourse to plausible noise, we perturb  $\tilde{x}$  by  $\epsilon$ . We call this type of perturbation “one-off noise” because it is applied only once to an entire recourse. This set-up is prevalent in existing work on robust recourse given their assumption that recourse is a one-step process itself. Following this setting, the magnitude of the plausible noise  $\sigma$  is neither affected by the size of recommended changes  $\delta$  nor by how a user progresses to  $\tilde{x}$  (i.e.,  $\mathcal{A}$ ); the distribution is realistic in so far as it should lie within the data manifold. We revise this assumption in Section 3.3.

To find a counterfactual instance that is robust to one-off plausible noise, we expect  $\tilde{x} + \epsilon$  to be classified as the counterfactual class. Such robustness can be measured

with Invalidation Rate (IR) which is defined in [Pawelczyk et al., 2023] as

$$\text{IR}(\tilde{x}) = \mathbb{E}_\epsilon[f(\tilde{x}) - f(\tilde{x} + \epsilon)] , \quad (2)$$

where the expectation is taken with respect to a random variable  $\epsilon$  controlled by the probability distribution  $p_{\tilde{x}}$  given in equation (1). We further derive a closed-form expression for the IR and its approximation in Proposition 1.

**Proposition 1.** *If  $K(\mathcal{X})$  is a smooth estimate of the probability density over  $\mathcal{X}$  – e.g., kernel density estimation – such that  $p_{\tilde{x}}$  is continuous, we can compute  $\text{IR}(\tilde{x})$  as*

$$\begin{aligned} \text{IR}(\tilde{x}) &= 1 - \int_{-\infty}^{\infty} 1 \cdot \mathbb{1}(f(x) = 1) \cdot p_{\tilde{x}}(x) dx - \int_{-\infty}^{\infty} 0 \cdot \mathbb{1}(f(x) = 0) \cdot p_{\tilde{x}}(x) dx \\ &= 1 - \int_{-\infty}^{\infty} f(x) \cdot p_{\tilde{x}}(x) dx . \end{aligned} \quad (3)$$

If  $p_{\tilde{x}}$  is discrete, we can approximate the expected IR through Monte Carlo Sampling as

$$\widetilde{\text{IR}}(\tilde{x}) = 1 - \frac{1}{N} \sum_{i=1}^N f(x_i) , \quad (4)$$

where  $x_i$  is sampled from the  $p_{\tilde{x}}$  distribution and  $N$  is the number of samples.

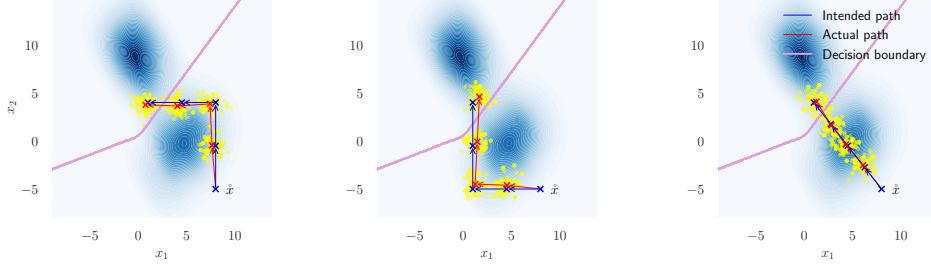
### 3.3 Accumulated Plausible Noise

When adding one-off noise, recourse is assumed to consist of a single step and the magnitude of noise is distance-agnostic. Recall that in [Pawelczyk et al., 2023] where  $\epsilon$  follows a normal distribution  $\mathcal{N}(0, \sigma^2 \mathbf{I})$ ,  $\sigma$  is set to be the same for every recourse. Under this assumption, increasing the salary level by \$500 is associated with the same degree of uncertainty as raising it by \$50,000. Similarly, Dominguez-Olmedo et al. [2022] and Virgolin and Fracaros [2023] add perturbations of the same size to different recourse regardless of the magnitude of their feature changes.

Here, we argue that noise – arising due to imperfect human implementation of recourse – accumulates along its path. Recall that in real-world settings a recourse involving sequential actions is often noisily implemented, and that humans tend to follow sequential instructions initially but fail to comply with them as time passes [Björkegren et al., 2020; DeGrandpre and Buskist, 1991; Hugtenburg et al., 2013]. Given the prevalence of such phenomena, we introduced a novel approach to algorithmically account for such user behaviour. Formally, we state that recourse implementation is vulnerable to the problem where the degree of adherence (or precise implementation) gradually decreases as the process gets longer.

In addition, recourse generation should consider the discreteness of actions and provide recourse as a series of actions [Verma et al., 2020]. As such, noise could arise when implementing every single action – the more actions a user needs to take, and the bigger changes each action entails, the more noise the entire process is likely to accumulate. For example, recourse that requires an increase of both salary and savings





(a) Increase  $x_2$  first, then decrease  $x_1$ .      (b) Decrease  $x_1$  first, then increase  $x_2$ .      (c) Change  $x_1$  and  $x_2$  at the same time.

**Fig. 3:** Recourse examples for a factual instance  $\hat{x}$  targeting the top-left desirable class patch. Actions can modify a single feature (a & b) or multiple features at each step (c), but it is desirable for an action to change a minimal set of features. Here, recourse is split into four discrete actions, which reflects how it is likely to be implemented in reality. The blue path shows the intended recourse trajectory when every action is implemented faithfully. The red path demonstrates the actual trajectory if every action is noisily implemented. For each action, we randomly sample 100 points from its plausible noise distribution and compute their mean, which yields a noise-aware step from which the follow-on actions are anchored. For demonstration purposes, we use the mean of plausible noise as the resulting state for each action, but in actual experiments, we allow the transition state to be sampled randomly from the noise distribution. The distribution of plausible noise associated with each action differs depending on the order of previous actions, which cumulatively affects the recourse trajectory. Hence, action orders should be considered when dealing with the robustness of recourse to noisy implementation of actions.

by \$50,000 would take longer to complete than the recourse that only affects one of these features, thus unforeseen circumstances are more likely to arise in the former case. Similarly, if savings are to be increased by only \$500 rather than \$50,000, such recourse becomes easier to implement and fewer uncertainties are expected. All such factors – captured in Proposition 2 – impact the ability of a user to faithfully implement recourse, with the *accumulated plausible noise* formalised in Definition 2.

**Proposition 2** (Accumulated Noise). *Assuming that noise can arise during the implementation of every recourse step, this noise would accumulate proportionally to the number of features changed and their magnitude required by every such step.*

**Definition 2** (Accumulated Plausible Noise). *For the recourse from  $\hat{x}$  to  $\check{x}$  that requires a series of actions  $\mathcal{A} = \{a_1, \dots, a_k\}$  where each action  $a_i \in \mathcal{A}$  is subject to*

noisy implementation, the accumulated noise distribution is

$$\begin{aligned}
\mathcal{N}_{(\hat{x}, \mathcal{A})}(\check{x}) &= \sum_{i=1}^k \epsilon_{s_i} + \check{x} \\
s.t. \quad \epsilon_{s_i} &= s'_i - s_i \quad s'_i \sim \mathcal{N}(s_i, \sigma_i^2 \mathbf{I}) \cdot K(\mathcal{X}) \\
s_i &\leftarrow s'_{i-1} \times a_i \quad \sigma_i^2 = \frac{\|a_i\|}{u} \times \sigma^2,
\end{aligned} \tag{5}$$

where  $u$  is the size unit of a standard action,  $\sigma^2$  is the magnitude of noise associated with an action of size  $u$ , and  $s_0 \equiv s'_0 \equiv \hat{x}$ .

From equation (5) we can also see that the distribution of  $s'_i$  depends on  $s_i$ , where  $s_i$  further depends on  $s'_{i-1}$  and  $a_i$ . Recursively,  $s'_{i-1}$  follows the probability distribution characterised by  $s_{i-1}$ , and the latter is influenced by  $s'_{i-2}$  and  $a_{i-1}$ . At the end, the distribution of the accumulated plausible noise is determined by the locations of intermediate points  $s_{1, \dots, k}$ , which are ultimately controlled by the order of actions in  $\mathcal{A}$ . Once  $s'_{i-1}$  and  $a_i$  are known,  $s_i$  can be set, then the distribution of  $s'_i$  is *conditionally independent* of all the previous actions  $a_{1, \dots, i-1}$  and past states  $s'_{1, \dots, i-2}$ . This shows that the noisy transition from one state to the next satisfies the Markov property, which is captured by Proposition 3.

**Proposition 3** (Markov Property of Noisy State Transition). *If the noise associated with each recourse action follows the plausible noise distribution, the distribution of the accumulated plausible noise depends upon the order and scale of said actions. Given the present  $s'_{i-1}$  and  $a_i$ , the subsequent  $\epsilon_{s_i}$  and  $s'_i$  do not depend on the past. In this case the noisy transition for  $s'_{i-1} \times a_i$  to  $s'_i$  satisfies the Markov property.*

We demonstrate the sub-optimal recourse-seeking processes in Fig. 3, which alter feature values in different orders, and show the importance of action orders to the distribution of accumulated plausible noise. Proofs of Proposition 2 and 3 are provided in Appendix D.

### 3.3.1 Evaluating Accumulated Noise

For a known action list  $\mathcal{A}$  guiding the recourse from  $\hat{x}$  to  $\check{x}$ , the Invalidation Rate is

$$\text{IR}_{\mathcal{A}}(\check{x}) = 1 - \int_{-\infty}^{\infty} f(x) \cdot p_x(\mathcal{N}_{(\hat{x}, \mathcal{A})}(\check{x})) d(x), \tag{6}$$

where the  $p_x$  function outputs the likelihood of  $x$  being drawn from the accumulated noise distribution. In a discrete setting,  $p_x$  is computed empirically via Monte Carlo Sampling. Note that this cannot be done by sampling random points from  $p_{\check{x}}$  (or  $p_{s_k}$ ) since  $p_{s_k}$  is non-deterministic unless the locations of all of its predecessors  $s'_{1, \dots, k-1}$  are fixed. To overcome this challenge we can repeat a complete implementation of  $\mathcal{A}$  multiple times where each time  $a_{1, \dots, k}$  is infused with randomly sampled plausible noise. Algorithm 1 offers details of this evaluation procedure.

---

**Algorithm 1** Assess accumulated plausible noise robustness.

---

**Require:**  $\hat{x}$ ,  $\tilde{x}$ ,  $\mathcal{X}$ , number of iterations  $M$ , set of actions  $\mathcal{A}$ , probability density function  $K$ , noise variance unit  $\sigma^2$ , action size unit  $u$ , classifier  $f$ , target class  $\tilde{y}$ .

**Ensure:**  $\text{IR}_{\mathcal{A}}(\tilde{x})$ .

```

{Sample plausible noise}
1: Function SampleNoise( $x, K, a, \sigma$ )
2:    $\text{var} \leftarrow \sigma^2 \times \frac{\|a_i\|}{u}$ 
3:    $B(x) \sim \mathcal{N}(x, \text{var} \cdot \mathbf{I}) \cdot K(\mathcal{X})$ 
4:   Return  $B(x)$ 
{Noisy implementation of an action}
5: Function NoisyStep( $\text{CurrState}, K, a, \sigma$ )
6:    $\text{NextState} \leftarrow \text{CurrState} \times a$ 
7:    $\text{NoiseSet} \leftarrow \text{SampleNoise}(\text{NextState}, K, a, \sigma)$ 
8:    $\text{NextStatePrime} \leftarrow \text{RandomChoice}(\text{NoiseSet})$ 
9:   Return  $\text{NextStatePrime}$ 
{Compute IR}
10:  $\text{count} \leftarrow 0$ 
11: for  $m = 0, \dots, M - 1$  do
12:    $\text{CurrState} \leftarrow \hat{x}$ 
13:   for  $a_i$  in  $\mathcal{A}$  do {Noisy implementation of  $\mathcal{A}$ }
14:      $\text{CurrState} \leftarrow \text{NoisyStep}(\text{CurrState}, K, a_i, \sigma)$ 
15:   end for
16:   if  $f(\text{CurrState}) = \tilde{y}$  then
17:      $\text{count} \leftarrow \text{count} + 1$ 
18:   end if
19: end for
20:  $\text{IR}_{\mathcal{A}}(\tilde{x}) \leftarrow \frac{\text{count}}{M}$ 

```

---

## 4 Generating Robust Sequential Recourse

In this section, we present a novel approach to address both the one-off plausible noise (introduced in Section 3.2) and accumulated plausible noise (proposed in Section 3.3) in algorithmic recourse. Motivated by the fact that recourse is a sequence of steps in which state transition satisfies Markov property (Proposition 3), we model the noisy human implementation of recourse as an MDP. We present our proposed method – ROBust SEquential (ROSE) recourse generator<sup>1</sup> – in Algorithm 2 and describe it in detail below.

### *State Space S*

Given that a dataset has both numerical (Num) and categorical (Cat) features, the state space of our MDP consists of the product of the continuous domains for numerical features ( $\mathbb{R}^{|\text{Num}|}$ ) and product of integer domains for categorical features ( $\mathbb{Z}^{\text{Cat}}$ ).

---

<sup>1</sup>Code: [https://github.com/xuanxuanxuan-git/sequential\\_cfe](https://github.com/xuanxuanxuan-git/sequential_cfe).

---

**Algorithm 2** MDP for robust algorithmic recourse.

---

**Require:** probability density function  $K$ , target class  $\tilde{y}$ , classifier  $f$ , invalidation rate function  $\text{IR}$ , noise variance unit  $\sigma^2$ , robustness threshold  $\tau$ , reward discount factor  $\gamma$ .

**Ensure:** MDP.

- 1: State space  $\mathbf{S} \subseteq \mathbb{R}^{|\text{Num}|} \times \mathbb{Z}^{|\text{Cat}|}$
  - 2: Actions  $\mathbf{A}(s) \subseteq \mathbf{A}$  for a state  $s \in \mathbf{S}$
  - 3:  $\mathcal{A} \leftarrow \emptyset$  {List of agent's executed actions}
  - 4: **Function Transition** ( $\text{CurrState}, K, a, \sigma, \mathcal{A}$ )
  - 5:   **if** AccumulatedNoise **then** {Noisy step}
  - 6:      $\text{NextState} \leftarrow \text{NoisyStep}(\text{CurrState}, K, a, \sigma)$
  - 7:   **else** {Precise step}
  - 8:      $\text{NextState} \leftarrow \text{CurrState} \times a$
  - 9:   **end if**
  - 10:    $\mathcal{A} \leftarrow \mathcal{A} \cup \{a\}$
  - 11:   **Return** NextState
  - 12: **Function Reward**( $\text{CurrState}, K, a, \sigma, \mathcal{A}$ )
  - 13:    $\text{NextState} \leftarrow \text{Transition}(\text{CurrState}, K, a, \sigma, \mathcal{A})$
  - 14:    $\text{InvRate} \leftarrow \text{IR}_{\mathcal{A}}(\text{NextState})$  {Use equation (6) for accumulated plausible noise, or equation (3) for one-off plausible noise.}
  - 15:   **if**  $f(\text{NextState}) = \tilde{y}$  and  $(\text{InvRate} < 1 - \tau)$  **then**
  - 16:      $\text{Reward} \leftarrow (1 - \text{InvRate}) \times \text{ConstantR}$  {ConstantR is a large constant reward.}
  - 17:   **else**
  - 18:      $\text{Reward} \leftarrow \text{softmax}(f(\text{NextState}))$
  - 19:   **end if**
  - 20:   **Return** Reward
  - 21: MDP  $\leftarrow \{\mathbf{S}, \mathbf{A}, \text{Transition}, \text{Reward}, \gamma\}$
- 

### *Action Space A*

Actions transition the environment from one state to another.  $\mathbf{A}(s)$  denotes all of the actions an agent can execute at state  $s \in \mathbf{S}$ . To facilitate action sparsity, we assume that each action  $a \in \mathbf{A}(s)$  corresponds to a modification of a single feature if this action is implemented faithfully.

### *Transition Function T*

The transition function outputs the state resulting from taking an action  $a$  at state  $s$ . If we assume that there is no noise in the transition, i.e., each action or feature change is implemented faithfully, then the exact feature change resulting from an action is added to the current state, yielding the next state (Line 8). On the other hand, if we assume that an action is executed with noise, then it leads to a random state sampled from a plausible noise set surrounding  $s \times a$  (Line 6). The former set-up supports the perturbation setting described in Section 3.2 where only a one-off noise is perturbed at  $\tilde{x}$ ; the latter case is applicable when addressing accumulated plausible noise outlined in Section 3.3.

### ***Reward Function***

Given the current state and action (as well as the list of implemented actions in the context of accumulated noise), the reward function returns a reward, taking into account whether the resulting state  $s'$  belongs to the desirable class  $\tilde{y}$  and how robust it is to the (accumulated) plausible noise. If the recourse is valid and its degree of robustness meets a certain threshold  $\tau$  – e.g., less than 25% of plausible noise is in the undesirable class for  $\tau = 0.75$  – then the reward equals to  $(1 - \text{InvRate})$  multiplied by a large constant reward `ConstantR` (Lines 15–16). If the desired robustness level has not been reached, only a small reward, which equals the probability of  $s'$  being classified as  $\tilde{y}$ , is returned. The small reward steers the algorithm towards a valid counterfactual and speeds up the computation.

### ***Additional Hyper-parameters***

The MDP contains a discount factor  $\gamma$ , which must be strictly less than 1 [Miller, 2022]. Setting  $\gamma$  to be less than 1 implicitly rewards shorter paths. Other parameters such as noise variance  $\sigma^2$  and robustness threshold  $\tau$  can be user-defined or domain-specific – we discuss their specific realisation in Section 5.

### ***Solving MDP Through Policy-gradient Method***

Once we have formulated the MDP, our goal is to find a policy  $\pi : \mathbf{S} \rightarrow \mathcal{A}$  that, given a state  $s \in \mathbf{S}$ , returns the best action  $a \in \mathcal{A}$  to take and gradually guides the agent from  $\hat{x}$  to  $\tilde{x}$ . We use existing policy-based deep reinforcement learning methods to approximate the optimal policy  $\pi$ . Compared with value-based methods, policy-based approaches have better performance when the state space  $\mathbf{S}$  or the action space  $\mathbf{A}$  are large [Miller, 2022]. Furthermore, policy-gradient methods outperform policy-iteration methods when  $\mathbf{S}$  or  $\mathbf{A}$  is continuous [Miller, 2022], which is exactly the case when modelling numerical features. We use the state-of-the-art policy-gradient method, Proximal Policy Optimisation (PPO), with Generalised Advantage Estimate (GAE) to learn the policy [Schulman et al., 2017, 2018].

## **5 Experimental Evaluation**

We evaluate ROSE against seven baseline methods on three real-world datasets. We further provide additional details about various hyper-parameter selection and implementation.

### **5.1 Methods**

**ROSE:** We set  $\gamma = 0.99$ , which implicitly encourages a shorter recourse. We further set `ConstantR` to 100 so that when a valid counterfactual is reached and the robustness level is satisfied, the agent receives a large reward. We test two variants of ROSE. ROSE-one applies a one-off plausible noise to  $\tilde{x}$  and follows the precise implementation of actions in  $\mathcal{A}$ . ROSE-mul(tiple) follows the noisy transition between states and relies on the accumulated plausible noise.

**Baselines:** We first compare ROSE against four non-robust baselines: Wachter, a gradient-based approach [Wachter et al., 2017]; Growing Sphere (GrSp), which is based

**Table 1:** ROSE evaluation. We report the average and standard deviation of each metric (except for efficacy) computed across all the chosen negative instances for each dataset. The best results across *all* methods are highlighted in bold; the best results across *robust-by-design* methods are underlined. Given the inherent trade-off between robustness and recourse distance, our method can achieve the highest robustness while effectively managing the distance. We use DiCE to generate one recourse per negative instance. We set  $r = 0.35$ ,  $\sigma^2 = 0.01$  and 30-second search timeout for PROBE. In CoGS, we allow features to decrease or increase by 0.1 after normalisation; we use  $m = 64$  to compute the  $\mathcal{K}$ -robustness score. We use the author’s recommended hyper-parameter settings in CROCO. ROSE-one and ROSE-mul use  $\sigma^2 = 0.01$  and  $\sigma^2 = 0.0005$  respectively, and  $\tau = 0.75$  as the robustness threshold.

|                 |                     | Metrics               |                                   |                                   |                           |                                   |                                   |                                   |
|-----------------|---------------------|-----------------------|-----------------------------------|-----------------------------------|---------------------------|-----------------------------------|-----------------------------------|-----------------------------------|
| Approach        | Efficacy $\uparrow$ | Sparsity $\downarrow$ | $\ell_1$ $\downarrow$             | Time (s) $\downarrow$             | Gaussian AIR $\downarrow$ | Plausible AIR $\downarrow$        | Acc AIR $\downarrow$              |                                   |
| German Credit   | Wachter             | <b>1.00</b>           | 20.00 $\pm$ 0.00                  | 0.46 $\pm$ 0.30                   | <b>0.020</b>              | 0.50 $\pm$ 0.04                   | 0.79 $\pm$ 0.16                   | 0.75 $\pm$ 0.17                   |
|                 | GrSp                | <b>1.00</b>           | 16.73 $\pm$ 0.44                  | 1.10 $\pm$ 0.78                   | <b>0.020</b>              | 0.43 $\pm$ 0.08                   | 0.77 $\pm$ 0.15                   | 0.77 $\pm$ 0.18                   |
|                 | DiCE                | <b>1.00</b>           | 7.78 $\pm$ 1.40                   | 1.12 $\pm$ 0.42                   | 0.176                     | 0.23 $\pm$ 0.16                   | 0.26 $\pm$ 0.22                   | 0.32 $\pm$ 0.20                   |
|                 | FastAR              | 0.93                  | <b>1.65 <math>\pm</math> 0.70</b> | <b>0.43 <math>\pm</math> 0.34</b> | 0.040                     | 0.43 $\pm$ 0.07                   | 0.54 $\pm$ 0.11                   | 0.51 $\pm$ 0.14                   |
|                 | CoGS                | <b>1.00</b>           | 6.98 $\pm$ 1.20                   | 0.50 $\pm$ 0.34                   | 1.971                     | 0.39 $\pm$ 0.04                   | 0.44 $\pm$ 0.11                   | 0.41 $\pm$ 0.14                   |
|                 | PROBE               | <b>1.00</b>           | 20.00 $\pm$ 0.00                  | 1.38 $\pm$ 0.80                   | 1.510                     | 0.24 $\pm$ 0.04                   | 0.66 $\pm$ 0.18                   | 0.70 $\pm$ 0.27                   |
|                 | CROCO               | 0.49                  | 20.00 $\pm$ 0.00                  | 1.37 $\pm$ 0.38                   | 0.283                     | <b>0.06 <math>\pm</math> 0.06</b> | 0.16 $\pm$ 0.13                   | 0.25 $\pm$ 0.13                   |
|                 | <i>ROSE-one</i>     | 0.82                  | 1.86 $\pm$ 0.84                   | 0.54 $\pm$ 0.33                   | 0.070                     | 0.14 $\pm$ 0.05                   | 0.22 $\pm$ 0.09                   | 0.28 $\pm$ 0.05                   |
|                 | <i>ROSE-mul</i>     | 0.71                  | 1.95 $\pm$ 0.92                   | 0.54 $\pm$ 0.32                   | 0.150                     | <b>0.06 <math>\pm</math> 0.02</b> | <b>0.10 <math>\pm</math> 0.04</b> | <b>0.23 <math>\pm</math> 0.02</b> |
|                 | Adult Income        | Wachter               | <b>1.00</b>                       | 6.00 $\pm$ 0.00                   | 0.29 $\pm$ 0.17           | 0.020                             | 0.50 $\pm$ 0.02                   | 0.75 $\pm$ 0.15                   |
| GrSp            |                     | <b>1.00</b>           | 6.46 $\pm$ 0.70                   | 0.70 $\pm$ 0.76                   | <b>0.005</b>              | 0.44 $\pm$ 0.08                   | 0.68 $\pm$ 0.16                   | 0.60 $\pm$ 0.17                   |
| DiCE            |                     | <b>1.00</b>           | 5.21 $\pm$ 0.71                   | 1.10 $\pm$ 0.51                   | 0.125                     | 0.18 $\pm$ 0.21                   | 0.36 $\pm$ 0.30                   | 0.45 $\pm$ 0.24                   |
| FastAR          |                     | <b>1.00</b>           | <b>1.00 <math>\pm</math> 0.00</b> | <b>0.09 <math>\pm</math> 0.05</b> | 0.010                     | 0.41 $\pm$ 0.07                   | 0.75 $\pm$ 0.14                   | 0.51 $\pm$ 0.18                   |
| CoGS            |                     | <b>1.00</b>           | 4.94 $\pm$ 0.29                   | 0.12 $\pm$ 0.06                   | 1.958                     | 0.41 $\pm$ 0.04                   | 0.76 $\pm$ 0.17                   | 0.56 $\pm$ 0.27                   |
| PROBE           |                     | 0.99                  | 12.98 $\pm$ 0.21                  | 12.24 $\pm$ 6.64                  | 9.770                     | 0.35 $\pm$ 0.02                   | 0.37 $\pm$ 0.40                   | 0.47 $\pm$ 0.19                   |
| CROCO           |                     | 0.99                  | 6.00 $\pm$ 0.00                   | 0.25 $\pm$ 0.05                   | 0.626                     | 0.09 $\pm$ 0.07                   | 0.54 $\pm$ 0.28                   | 0.26 $\pm$ 0.25                   |
| <i>ROSE-one</i> |                     | <b>1.00</b>           | 1.06 $\pm$ 0.24                   | 0.18 $\pm$ 0.06                   | 0.030                     | <b>0.05 <math>\pm</math> 0.02</b> | <b>0.19 <math>\pm</math> 0.07</b> | 0.11 $\pm$ 0.11                   |
| <i>ROSE-mul</i> |                     | <b>1.00</b>           | 1.02 $\pm$ 0.14                   | 0.22 $\pm$ 0.12                   | 0.150                     | 0.08 $\pm$ 0.03                   | 0.26 $\pm$ 0.10                   | <b>0.04 <math>\pm</math> 0.06</b> |
| COMPAS          |                     | Wachter               | <b>1.00</b>                       | 4.00 $\pm$ 0.00                   | 0.19 $\pm$ 0.15           | 0.020                             | 0.47 $\pm$ 0.03                   | 0.79 $\pm$ 0.10                   |
|                 | GrSp                | <b>1.00</b>           | 4.05 $\pm$ 0.21                   | 0.25 $\pm$ 0.30                   | <b>0.005</b>              | 0.48 $\pm$ 0.03                   | 0.75 $\pm$ 0.10                   | 0.66 $\pm$ 0.13                   |
|                 | DiCE                | <b>1.00</b>           | 3.28 $\pm$ 0.64                   | 0.84 $\pm$ 0.51                   | 0.063                     | 0.10 $\pm$ 0.13                   | 0.21 $\pm$ 0.16                   | 0.31 $\pm$ 0.13                   |
|                 | FastAR              | <b>1.00</b>           | <b>1.00 <math>\pm</math> 0.00</b> | <b>0.03 <math>\pm</math> 0.01</b> | 0.050                     | 0.14 $\pm$ 0.14                   | 0.15 $\pm$ 0.14                   | 0.05 $\pm$ 0.11                   |
|                 | CoGS                | <b>1.00</b>           | 2.88 $\pm$ 0.32                   | 0.23 $\pm$ 0.12                   | 1.323                     | 0.27 $\pm$ 0.02                   | 0.29 $\pm$ 0.15                   | 0.22 $\pm$ 0.15                   |
|                 | PROBE               | <b>1.00</b>           | 6.99 $\pm$ 0.10                   | 0.53 $\pm$ 0.31                   | 1.390                     | 0.33 $\pm$ 0.02                   | 0.73 $\pm$ 0.11                   | 0.65 $\pm$ 0.16                   |
|                 | CROCO               | <b>1.00</b>           | 4.00 $\pm$ 0.00                   | 0.41 $\pm$ 0.14                   | 0.486                     | 0.10 $\pm$ 0.01                   | 0.12 $\pm$ 0.12                   | 0.05 $\pm$ 0.07                   |
|                 | <i>ROSE-one</i>     | <b>1.00</b>           | <b>1.00 <math>\pm</math> 0.00</b> | 0.04 $\pm$ 0.02                   | 0.610                     | 0.10 $\pm$ 0.08                   | 0.11 $\pm$ 0.08                   | <b>0.01 <math>\pm</math> 0.03</b> |
|                 | <i>ROSE-mul</i>     | <b>1.00</b>           | <b>1.00 <math>\pm</math> 0.00</b> | 0.04 $\pm$ 0.02                   | 0.620                     | <b>0.09 <math>\pm</math> 0.08</b> | <b>0.10 <math>\pm</math> 0.08</b> | <b>0.01 <math>\pm</math> 0.03</b> |

on a random search algorithm [Laugel et al., 2018]; DiCE, which generates a diverse set of counterfactual explanations through gradient descent [Mothilal et al., 2020]; and FASTAR, which generates sequential recourse through policy-based reinforcement learning [Verma et al., 2022]. The former three methods assume an instantaneous, one-step implementation of the counterfactual explanation, whereas the latter one accounts for the order of actions. Furthermore, we evaluate three methods that are designed to generate recourse that is robust to perturbations affecting  $\tilde{x}$ : CoGS is an evolutionary algorithm that distinguishes perturbations affecting features that are included in the counterfactuals and the remaining ones [Virgolin and Fracaros, 2023]; PROBE uses gradient descent optimisation to generate robust recourse in the presence of noisy human implementation [Pawelczyk et al., 2023]; and CROCO leverages a new estimator of soft recourse invalidation rate that provides a theoretical guarantee on the true recourse robustness [Guyomard et al., 2023]. We also experimented with ARAR [Dominguez-Olmedo et al., 2022], and found that it is only compatible with linear classifiers such as logistic regression; its efficacy is as low as 0.02 when the classifier is a neural network. With logistic regression, ARAR provides recourse with their  $\ell_1$  distance up to ten times higher than those by ROSE, thus impractical for users to follow. A similar finding about ARAR is reported in [Pawelczyk et al., 2023]. For brevity, we do not report its performance in this work. All methods use  $\ell_1$ -norm as the distance function.

## 5.2 Datasets and Classifiers

We consider three real-world datasets: German Credit [Hofmann, 1994], Adult Income [Becker and Kohavi, 1996] and COMPAS [Larson et al., 2016]. Each dataset has a desirable class labelled 1, and an undesirable class labelled 0. Following best practice [Pawelczyk et al., 2023], all the datasets were normalised so that  $x \in [0, 1]^d$ . For prediction models, we train a neural network with a 50-neuron hidden layer and ReLU activation. All recourse was generated with respect to these classifiers. We use the learning rate of 0.002, batch size of 50, and 100 training epochs for all datasets. We split the datasets into 80%–20% parts used respectively for training and evaluation. Given that the German Credit dataset is small, we generate recourse for all the data instances that are predicted as the undesirable class – hereafter referred to as *negative instances* – yielding 257 points. Contrarily, the Adult dataset is large, making it computationally expensive for some baselines to output recourse for all the negative instances. To address this issue we randomly choose 200 negative instances from the test set for recourse generation. For COMPAS, we generate recourse for all the 104 negative instances in the test set.

## 5.3 Measures

We leverage evaluation metrics established in the literature to measure method performance [Verma et al., 2022; Pawelczyk et al., 2023]. Specifically, we report *efficacy* – the fraction of negative instances for which an explainer can successfully generate valid recourse; *sparsity* – the number of features that need to be changed to achieve

the recourse; and  $\ell_1$  distance between  $\hat{x}$  and  $\check{x}$ . To evaluate the complexity empirically, we report the *time* taken to generate recourse for a single instance.

We also check if an explainer is robust to Gaussian noise and plausible noise, which is measured in current literature using *Average Invalidation Rate (AIR)* – the probability of obtaining a counterfactual with an undesirable class, when small changes (sampled from varying noise distribution) are applied to it [Pawelczyk et al., 2023; Guyomard et al., 2023]. To generate (one-off) Gaussian noise, we randomly sample 1,000 points from a Gaussian distribution  $\mathcal{N}(0, \sigma^2 \mathbf{I})$  as  $\epsilon$  for each  $\check{x}$ , then compute IR (as described in equation (2)) across all instances, and report *Gaussian AIR*. Similarly, for (one-off) plausible noise, we sample 1,000 points from the  $\mathcal{N}(\check{x}, \sigma^2 \mathbf{I}) \cdot K(\mathcal{X})$  distribution and report *Plausible AIR*. In both experiments we set  $\sigma^2 = 0.01$ . When evaluating accumulated noise, we use 5% of the size of the one-off noise (i.e.,  $\sigma^2 = 0.0005$ ) as the noise added to each unit of action. We set the size of the action unit  $u = 0.025$  so that the closest recourse  $\delta = 0.03$  contains at least one action unit. For non-sequential methods we assume that the actions (i.e., feature changes) are executed in a random order since these approaches do not output this information. For sequential explainers we follow the output action order. We run the evaluation procedure outlined in Algorithm 1 1,000 times and report *Acc AIR*.

## 5.4 Implementation Details

We use off-the-shelf implementation of the PPO with GAE algorithm [Kostrikov, 2018] to solve the MDP problem and use OpenAI Gym library [Brockman et al., 2016] to create the environment for each dataset. In the PPO algorithm, both actor and critic are approximated by fully connected neural networks with two hidden layers of 64 neurons. We strictly follow the hyper-parameter set-ups used in [Verma et al., 2022] and the best practice of using random data instances from the training set as the starting point for training [Verma et al., 2022]. The training time for each dataset was 30 minutes and one hour for ROSE-one and ROSE-mul respectively. We use a CPU machine for training since the GPU cannot accelerate the most time-consuming computation of calculating IR.

## 5.5 Results

It has been proven theoretically that CE methods face an inherent trade-off between their robustness and other desired properties, i.e., increasing robustness of CEs results in a drop of other metrics [Pawelczyk et al., 2023; Guyomard et al., 2023]. Therefore, it is critical for recourse generators to effectively manage such trade-off. The experimental results suggest that our method outperforms all other robustness-oriented methods across almost all the metrics and offers the best level of robustness among non-robust approaches, albeit with a slight penalty to the other metrics.

The performance of all generators is reported in Table 1. For each dataset, the first four methods generate non-robust recourse and the last five approaches generate recourse that is robust to different types of perturbations. We see that either ROSE-one or ROSE-mul achieves the lowest invalidation rate across all the datasets on

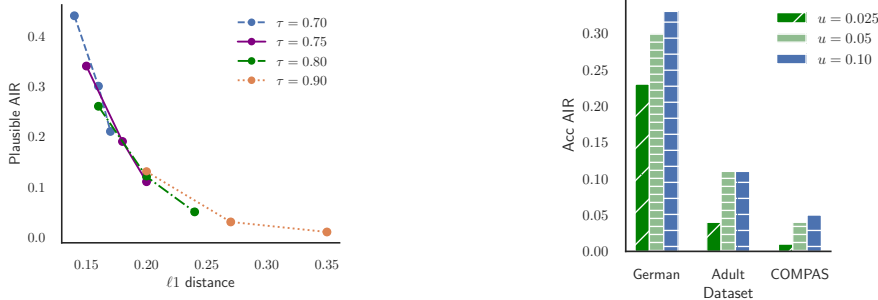


Gaussian noise, plausible noise and accumulated plausible noise. Compared with *non-robust* methods, the robustness of ROSE comes at an additional cost of either worse efficacy (for German Credit) or increased computation time. On the other hand, the  $\ell_1$  distance of recourse output by ROSE is comparable with that generated by gradient-based approaches and GrSp for German Credit, and notably smaller in Adult Income and COMPAS. FastAR always produces the shortest recourse with little robustness to any noise; this corresponds to the inherent trade-off between recourse cost and robustness. Moreover, unlike the gradient-based optimisation methods which modify almost all features, ROSE maintains low sparsity and tends to alter only one or two features across all the datasets.

Next, we compare our method ROSE with the *robust-by-design* methods: CoGS, PROBE and CROCO. We always achieve the lowest sparsity, the shortest computation time (except on COMPAS) and superior robustness for all types of perturbations. ROSE’s  $\ell_1$  distance is the shortest on COMPAS and slightly higher than CoGS on German Credit and Adult Income. This suggests that ROSE can more effectively manage the trade-off between the recourse robustness and cost. On the other hand, CoGS produces shorter recourse with a high invalidation rate. PROBE has the highest or second highest efficacy across all datasets, but its recourse generation time is significantly longer. CROCO produces relatively proximate recourse in a short time but has a high sparsity. It is also more robust to Gaussian noise than CoGS or PROBE, but less robust than ROSE under every noise distribution. The results also indicate that guarding against Gaussian noise does not guarantee robustness to plausible noise, even though we used the same  $\sigma^2$  value for both types of one-off noise. This is because adapting the Gaussian noise to the local data geometry reshapes the noise distribution, possibly making it significantly different from the normal distribution. In Adult Income, for example, PROBE’s AIR to Gaussian noise and plausible noise are comparable, but in German Credit and COMPAS plausible AIR is more than double Gaussian AIR. We find that ROSE-one is robust to plausible noise and at the same time keeps the Gaussian AIR at a low level.

In terms of the accumulated plausible noise, ROSE-mul always achieves the lowest Acc AIR while at the same time being relatively robust to one-off noise. However, in the German Credit dataset we note that its lower AIR comes at a cost of efficacy and sparsity. Further, ROSE-mul generally takes more time to generate robust recourse than ROSE-one and the other non-robust explainers. It is also worth noting that robustness to one-off noise does not imply robustness to accumulated noise. Specifically, the Acc AIR of PROBE is almost as high as that of non-robust methods. This is because PROBE always sacrifices distance for robustness to one-off noise but disregards the fact that the longer the recourse, the more uncertainty there is, thus it generally produces longer recourse that can accumulate a large amount of noise.

In summary, we find that ROSE has the lowest invalidation rate across all datasets for all types of perturbations among the non-robust recourse methods, while providing the sparsest and short recourse among the robust recourse methods in short computation time.



(a) For each  $\tau$ , we set  $\sigma^2 \in \{0.005, 0.01, 0.015\}$  from left to right.

(b) We keep  $\sigma^2 = 0.005$  and  $\tau = 0.75$  when varying  $u$  for each dataset.

**Fig. 4:** Panel (a) shows the effect of different  $\tau$  and  $\sigma^2$  when generating robust sequential recourse with ROSE-one for the Adult Income dataset. Panel (b) shows the effect of different  $u$  on the robustness of recourse with ROSE-mul.

## 5.6 Impact of Hyper-parameters of ROSE

We further study different hyper-parameters used by ROSE to generate robust recourse. In these experiments, recourse is evaluated against the same scale of noise perturbation as described in Section 5.3.

### *One-off Plausible Noise*

We investigate the effects of  $\tau$  and  $\sigma^2$  for ROSE-one to generate robust recourse. Fig. 4a illustrates that higher  $\tau$  and higher  $\sigma^2$  lead to lower AIR thus greater robustness. In these experiments, the efficacy remains 100% on the Adult Income dataset. Note that we only experiment with  $\tau$  up to 0.9, as setting  $\tau$  greater than 0.9 would further sacrifice efficacy. Our results on Adult Income are representative of experiments on the other two datasets.

### *Accumulated Plausible Noise*

We also study the impacts of  $u$ ,  $\tau$  and  $\sigma^2$  in ROSE-mul. We find that a smaller  $u$  leads to higher robustness (Fig. 4b) but a longer distance. The reason is that, with smaller  $u$ , each action is assumed to bring smaller feature changes, thus more actions are needed to complete the recourse; as a result, noise is added more frequently.  $\sigma^2$  and  $\tau$  have the same effect on ROSE-one and ROSE-mul.

### *Different Classifiers*

We further investigate ROSE’s performance when pairing with linear classifiers, e.g., logistic regression. We find that the performance of ROSE-one and ROSE-mul do not vary significantly across classifiers, and they consistently outperform all baselines in terms of robustness and sparsity while effectively managing recourse costs and computation time; for brevity we omit the results here.

Lastly, we evaluate the robustness of recourse to *varying magnitude of perturbation* while keeping the hyper-parameters used in each method the same as in Table 1. We find that as  $\sigma^2$  and  $u$  used in evaluation get larger, recourse is perturbed with more noise, consequently AIR of all methods increases. ROSE-one or ROSE-mul still maintain the lowest AIR across all experiments. We include the complete set of experimental results in Appendix B.

## 6 Conclusion

Uncertainty and sub-optimal human implementation of algorithmic recourse are inevitable. When recourse gets longer and more feature changes are required, the process gets more complex and harder for users to implement. As such, they are less likely to faithfully implement the recommended feature changes. In this paper we argue that the noise affecting recourse – which captures real-world noisy human actions – should be plausible and compatible with the underlying data manifold. In addition, noise accumulates as recourse gets longer, reflecting the increasing difficulty and uncertainty in its implementation. To address these challenges we formulate robust sequential recourse generation as an MDP problem and use policy-based reinforcement learning to generate robust recourse. Our method ROSE accounts for both one-off plausible noise and accumulated plausible noise. It generates a sequence of actions and ensures that even if they are not implemented faithfully, i.e., the actual feature changes resulting from user actions are different from the ones prescribed by an explanation, they can still lead to the desired outcome.

**Supplementary information.** Not applicable.

**Acknowledgements.** Not applicable.

## Declarations

**Funding.** This research was conducted by the ARC Centre of Excellence for Automated Decision-Making and Society (project number CE200100005), funded by the Australian Government through the Australian Research Council. Additional support was provided by the Hasler Foundation (grant number 23082).

**Competing Interests.** We declare no competing interests.

**Ethics Approval and Consent to Participate.** Not applicable.

**Consent for Publication.** Not applicable.

### Data Availability.

*German Credit:* <https://archive.ics.uci.edu/dataset/144/statlog+german+credit+data>.

*Adult Income:* <https://archive.ics.uci.edu/dataset/2/adult>.

*COMPAS:* <https://github.com/propublica/compas-analysis>.

**Materials Availability.** Not applicable.

**Code Availability.** [https://github.com/xuanxuanxuan-git/sequential\\_cfe](https://github.com/xuanxuanxuan-git/sequential_cfe)

## References

- Barocas, S., A.D. Selbst, and M. Raghavan 2020. The hidden assumptions behind counterfactual explanations and principal reasons. In *Proceedings of the 2020 conference on fairness, accountability, and transparency*, pp. 80–89.
- Becker, B. and R. Kohavi. 1996. Adult. UCI Machine Learning Repository. DOI: <https://doi.org/10.24432/C5XW20>.
- Björkegren, D., J.E. Blumenstock, and S. Knight. 2020. Manipulation-proof machine learning. *arXiv preprint arXiv:2004.03865* .
- Brockman, G., V. Cheung, L. Pettersson, J. Schneider, J. Schulman, J. Tang, and W. Zaremba. 2016. Openai gym.
- Dandl, S., C. Molnar, M. Binder, and B. Bischl 2020. Multi-objective counterfactual explanations. In *Parallel Problem Solving from Nature–PPSN XVI: 16th International Conference, PPSN 2020, Leiden, The Netherlands, September 5-9, 2020, Proceedings, Part I*, pp. 448–469. Springer.
- DeGrandpre, R.J. and W.F. Buskist. 1991. Effects of accuracy of instructions on human behavior: Correspondence with reinforcement contingencies matters. *The Psychological Record* 41: 371–384 .
- Dominguez-Olmedo, R., A.H. Karimi, and B. Schölkopf 2022. On the adversarial robustness of causal algorithmic recourse. In *International Conference on Machine Learning*, pp. 5324–5342. PMLR.
- Downs, M., J.L. Chu, Y. Yacoby, F. Doshi-Velez, and W. Pan. 2020. CRUDS: Counterfactual recourse using disentangled subspaces. *ICML WHI 2020*: 1–23 .
- Ferrario, A. and M. Loi. 2022. The robustness of counterfactual explanations over time. *IEEE Access* 10: 82736–82750 .
- Guyomard, V., F. Fessant, T. Guyet, T. Bouadi, and A. Termier 2023. Generating robust counterfactual explanations. In *Joint European Conference on Machine Learning and Knowledge Discovery in Databases*, pp. 394–409. Springer.
- Hofmann, H. 1994. Statlog (German Credit Data). UCI Machine Learning Repository. DOI: <https://doi.org/10.24432/C5NC77>.
- Hugtenburg, J.G., L. Timmers, P.J. Elders, M. Vervloet, and L. van Dijk. 2013. Definitions, variants, and causes of nonadherence with medication: A challenge for tailored interventions. *Patient preference and adherence*: 675–682 .
- Jiang, J., A. Rago, F. Leofante, and F. Toni. 2024. Recourse under model multiplicity via argumentative ensembling. *The 23rd International Conference on Autonomous Agents and Multi-Agent Systems* .

- Joshi, S., O. Koyejo, W. Vijitbenjaronk, B. Kim, and J. Ghosh. 2019. Towards realistic individual recourse and actionable explanations in black-box decision making systems. *arXiv preprint arXiv:1907.09615* .
- Kanamori, K., T. Takagi, K. Kobayashi, Y. Ike, K. Uemura, and H. Arimura 2021. Ordered counterfactual explanation by mixed-integer linear optimization. In *Proceedings of the AAAI Conference on Artificial Intelligence*, Volume 35, pp. 11564–11574.
- Karimi, A.H., G. Barthe, B. Balle, and I. Valera 2020. Model-agnostic counterfactual explanations for consequential decisions. In *International Conference on Artificial Intelligence and Statistics*, pp. 895–905. PMLR.
- Kostrikov, I. 2018. Pytorch implementations of reinforcement learning algorithms. <https://github.com/ikostrikov/pytorch-a2c-ppo-acktr-gail>.
- Larson, J., S. Mattu, L. Kirchner, and J. Angwin. 2016. How we analyzed the COMPAS recidivism algorithm. *ProPublica* .
- Laugel, T., M.J. Lesot, C. Marsala, X. Renard, and M. Detyniecki 2018. *Comparison-Based Inverse Classification for Interpretability in Machine Learning*, pp. 100–111. Springer International Publishing.
- Miller, T. 2022. *Introduction to Reinforcement Learning*.
- Mothilal, R.K., A. Sharma, and C. Tan 2020. Explaining machine learning classifiers through diverse counterfactual explanations. In *Proceedings of the 2020 conference on fairness, accountability, and transparency*, pp. 607–617.
- Naumann, P. and E. Ntoutsis 2021. *Consequence-Aware Sequential Counterfactual Generation*, pp. 682–698. Springer International Publishing.
- Pawelczyk, M., K. Broelemann, and G. Kasneci 2020a. Learning model-agnostic counterfactual explanations for tabular data. In *Proceedings of The Web Conference 2020*, pp. 3126–3132.
- Pawelczyk, M., K. Broelemann, and G. Kasneci 2020b. On counterfactual explanations under predictive multiplicity. In *Conference on Uncertainty in Artificial Intelligence*, pp. 809–818. PMLR.
- Pawelczyk, M., T. Datta, J. van-den Heuvel, G. Kasneci, and H. Lakkaraaju 2023. Probabilistically robust recourse: Navigating the trade-offs between costs and robustness in algorithmic recourse. In *11th International Conference on Learning Representations (ICLR)*.
- Poyiadzi, R., K. Sokol, R. Santos-Rodriguez, T. De Bie, and P. Flach 2020. FACE: Feasible and actionable counterfactual explanations. In *Proceedings of the AAAI/ACM*

- Conference on AI, Ethics, and Society*, pp. 344–350.
- Ramakrishnan, G., Y.C. Lee, and A. Albarghouthi 2020. Synthesizing action sequences for modifying model decisions. In *Proceedings of the AAAI Conference on Artificial Intelligence*, Volume 34, pp. 5462–5469.
- Raman, N., D. Magazzeni, and S. Shah 2023. Bayesian hierarchical models for counterfactual estimation. In *International Conference on Artificial Intelligence and Statistics*, pp. 1115–1128. PMLR.
- Rawal, K., E. Kamar, and H. Lakkaraju. 2020. Algorithmic recourse in the wild: Understanding the impact of data and model shifts. *arXiv preprint arXiv:2012.11788* .
- Russell, C. 2019. Efficient search for diverse coherent explanations. In *Proceedings of the Conference on Fairness, Accountability, and Transparency*, pp. 20–28.
- Schulman, J., P. Moritz, S. Levine, M. Jordan, and P. Abbeel. 2018. High-dimensional continuous control using generalized advantage estimation.
- Schulman, J., F. Wolski, P. Dhariwal, A. Radford, and O. Klimov. 2017. Proximal policy optimization algorithms.
- Sharma, S., A.H. Gee, J. Henderson, and J. Ghosh. 2022. Faster-ce: fast, sparse, transparent, and robust counterfactual explanations. *arXiv preprint arXiv:2210.06578* .
- Slack, D., A. Hilgard, H. Lakkaraju, and S. Singh. 2021. Counterfactual explanations can be manipulated. *Advances in neural information processing systems* 34: 62–75 .
- Tsirtsis, S., A. De, and M. Rodriguez. 2021. Counterfactual explanations in sequential decision making under uncertainty. *Advances in Neural Information Processing Systems* 34: 30127–30139 .
- Tsirtsis, S. and M. Rodriguez. 2024. Finding counterfactually optimal action sequences in continuous state spaces. *Advances in Neural Information Processing Systems* 36 .
- Upadhyay, S., S. Joshi, and H. Lakkaraju. 2021. Towards robust and reliable algorithmic recourse. *Advances in Neural Information Processing Systems* 34: 16926–16937 .
- Ustun, B., A. Spangher, and Y. Liu 2019. Actionable recourse in linear classification. In *Proceedings of the conference on fairness, accountability, and transparency*, pp. 10–19.
- Van Looveren, A. and J. Klaise 2021. Interpretable counterfactual explanations guided by prototypes. In *Machine Learning and Knowledge Discovery in Databases*.

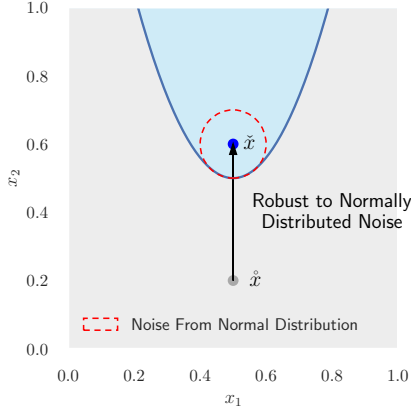
*Research Track: European Conference, ECML PKDD 2021, Bilbao, Spain, September 13–17, 2021, Proceedings, Part II 21*, pp. 650–665. Springer.

Verma, S., V. Boonsanong, M. Hoang, K.E. Hines, J.P. Dickerson, and C. Shah. 2020. Counterfactual explanations and algorithmic recourses for machine learning: A review. *arXiv preprint arXiv:2010.10596* .

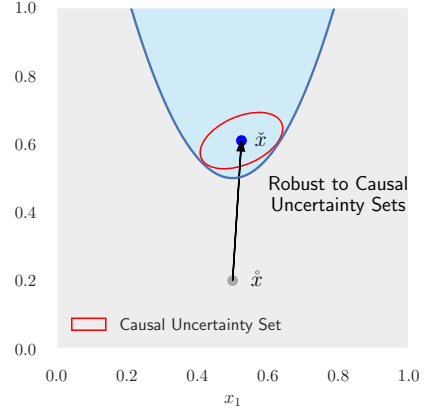
Verma, S., K. Hines, and J.P. Dickerson 2022. Amortized generation of sequential algorithmic recourses for black-box models. In *Proceedings of the AAAI Conference on Artificial Intelligence*, Volume 36, pp. 8512–8519.

Virgolin, M. and S. Fracaros. 2023. On the robustness of sparse counterfactual explanations to adverse perturbations. *Artificial Intelligence* 316: 103840 .

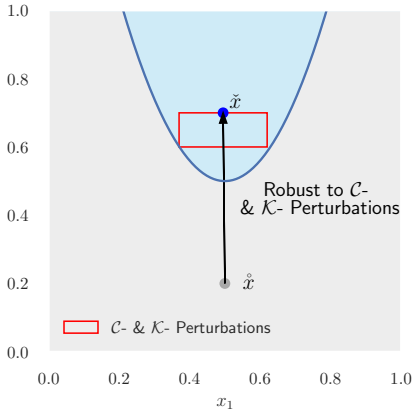
Wachter, S., B. Mittelstadt, and C. Russell. 2017. Counterfactual explanations without opening the black box: Automated decisions and the GDPR. *Harv. JL & Tech.* 31: 841 .



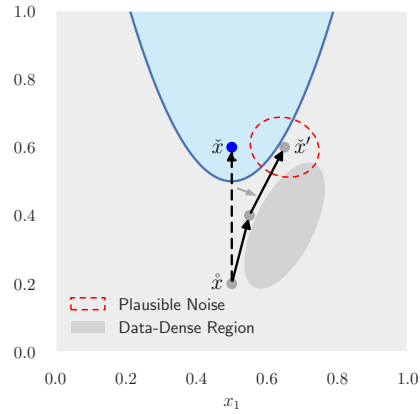
(a) Noise sampled from normal distribution [Pawelczyk et al., 2023].



(b) Noise that follows a causal model [Dominguez-Olmedo et al., 2022].



(c) Noise sampled from a manually defined range [Virgolin and Fracaros, 2023].



(d) Plausible noise adapted to local data geometry (our work).

**Fig. A1:** Various ways to represent human’s noisy implementation of algorithmic recourse. In (a) and (d), noise around  $\tilde{x}$  (shown in dotted lines) follows a probability distribution. In (b) and (c), the shape of the noise distribution (shown in solid lines) has to be manually defined. In addition, it is assumed that the occurrence of noise inside the solid region is equally possible regardless of their distance to  $\tilde{x}$ .



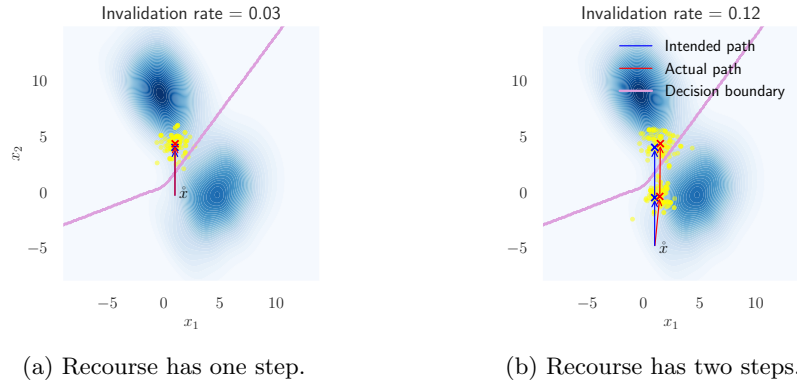


**Fig. A2:** Two recourse with varying length for a factual instance  $\hat{x}$  targeting the top-left desirable class patch. The length of recourse in (b) is double the length of recourse in (a). In (b), the noisy state after the first step is determined by sampling from a plausible noise distribution and using the mean as the new starting state for the subsequent action.

## Appendix A Various Types of Perturbations

As discussed in Section 2, current literature about robust recourse has inconsistent formulations of adversarial perturbations, especially of perturbations on individual data instances. In this section, we summarise different representations of noise used in the most recent work. We provide the pictorial representations of robust recourse in Figure A1.

Pawelczyk et al. [2023] proposed that recourse should be robust to noisy human implementation. To model the noise in human implementation, they perturbed the recourse for a negative data instance by a random variable  $\epsilon$  which is drawn from a Gaussian probability distribution (i.e.,  $\epsilon \sim \mathcal{N}(0, \sigma^2 \mathbf{I})$ ), as shown in Figure A1a. However, they assumed the same magnitude of uncertainty in recourse regardless of how difficult it is to achieve the recourse. Plausibility was not considered either in their work.

Dominguez-Olmedo et al. [2022] argued that robust recourse should guide *all* instances in the uncertainty set around  $\hat{x}$  to the same desirable prediction outcome. The uncertainty set (i.e., perturbations) includes all of the plausible data points similar to  $\hat{x}$ , as shown in Figure A1b. To model the plausibility of noise, they explicitly took into account the *linear* causal relationships between features when creating the perturbation set, provided that the underlying causal model is known or can be approximated well. As such, the distribution of the noise is re-shaped to accommodate the linear causal model. Unlike Gaussian noise in Figure A1a which follows a probability distribution, the uncertainty set in Figure A1b assumes that the occurrences of instances within this set are equally possible.

Similarly, Virgolin and Fracaros [2023] accounted for unforeseen circumstances when generating recourse. They manually defined the perturbation ranges for each

feature in their experiment dataset based on their domain knowledge. They further broke down the perturbations into two types: perturbations to features that need to be acted upon when implementing the recourse, and perturbations to features that should remain the same when pursuing the recourse. On an abstract level, the perturbation set can be modelled as a hyper-box (Figure A1c) which contains all possible combinations of feature values within their perturbation ranges. Similar to the causal noise, they also assumed that all instances from this perturbation set are equally possible to happen.

In this work, we model the sub-optimal recourse implementation and simultaneously consider the plausibility of noisy implementation and accumulated uncertainty. To do so, we associate the magnitude of noise with the number of actions and the scale thereof in a recourse. As shown in Figure A1d, we assume that the recourse takes two steps/actions to complete, and each action might be executed imperfectly. Thus, after taking the first action, the intermediate state could land in a position different from the intended place. When determining the likely positions of any intermediate states, we consider the plausibility of their distribution, i.e., they follow plausible noise distribution. We argue that such plausible noise accumulates as the recourse gets longer, and recourse should be robust to such increasing uncertainty. We also implement the idea shown in Figure A1d on a synthetic dataset and compute the invalidation rate for plausible noise added to the recourse of varying length. As shown in Figure A2, each unit of action is perturbed with the same magnitude of plausible noise. Recourse in Figure A2a is shorter so plausible noise is only added once. As a result, its invalidation rate is 0.03. On the other hand, the length of recourse in Figure A2b is double that of in Figure A2a, so plausible noise is added twice – one to each step. As a result, the invalidation rate is 0.12. Note that the actual path in Figure A2b leans towards the bottom-right patch of data points, whereas the actual path in Figure A2a is less affected by this cluster of data.

## Appendix B Additional Experiments

### B.1 Different Hyper-Parameter Values in ROSE

In this section, we report the performance of ROSE under different hyper-parameter values in its recourse generation. Specifically, when generating robust recourse, ROSE uses  $\sigma^2$  and  $\tau$  to control the magnitude of noise that recourse should be robust to and the degree of robustness adherence, respectively. Once recourse is generated, we evaluate them using the same magnitude of noise.

#### B.1.1 One-off Plausible Noise

Figure 4a shows the results of Average Invalidation Rate (AIR) and  $\ell_1$  distance when different robustness threshold  $\tau$  and different variance of plausible noise distribution  $\sigma^2$  are used in ROSE-one to generate robust recourse. We can empirically observe that a lower AIR is achieved at the cost of  $\ell_1$  distance. In other words, the longer the recourse, the more robust the recourse is to one-off plausible noise. Additionally, higher  $\tau$  and higher  $\sigma^2$  lead to lower AIR and greater robustness. In these experiments, the efficacy remains 100% on the Adult Income dataset. We also observe a similar trade-off from results on the German Credit and COMPAS datasets. Note that we

**Table B1:** Different  $\sigma^2$  and  $u$  used in ROSE-mul to generate robust recourse. When varying  $\sigma^2$ , we keep  $u = 0.025$ ; when varying  $u$ , we keep  $\sigma^2 = 5\%$ . Results of ROSE-mul in this table are complementary to results in Table 1. When evaluating IR for the accumulated noise, we perturb recourse using the same size of noise set-up –  $\sigma^2 = 0.0005, u = 0.025$ .

|                  |                   | Metrics             |                       |                       |                       |                      |
|------------------|-------------------|---------------------|-----------------------|-----------------------|-----------------------|----------------------|
|                  |                   | Efficacy $\uparrow$ | Sparsity $\downarrow$ | $\ell_1$ $\downarrow$ | Time (s) $\downarrow$ | Acc AIR $\downarrow$ |
| German<br>Credit | $\sigma^2 = 3\%$  | 0.75                | $1.82 \pm 0.88$       | $0.49 \pm 0.32$       | 0.171                 | $0.26 \pm 0.20$      |
|                  | $\sigma^2 = 7\%$  | 0.72                | $1.84 \pm 0.92$       | $0.48 \pm 0.34$       | 0.173                 | $0.21 \pm 0.15$      |
|                  | $\sigma^2 = 10\%$ | 0.70                | $1.83 \pm 0.90$       | $0.49 \pm 0.25$       | 0.185                 | $0.19 \pm 0.18$      |
|                  | $u = 0.05$        | 0.78                | $1.71 \pm 0.85$       | $0.47 \pm 0.33$       | 0.160                 | $0.30 \pm 0.19$      |
|                  | $u = 0.10$        | 0.81                | $1.71 \pm 0.82$       | $0.44 \pm 0.32$       | 0.147                 | $0.33 \pm 0.28$      |
| Adult<br>Income  | $\sigma^2 = 3\%$  | 1.00                | $1.07 \pm 0.26$       | $0.22 \pm 0.09$       | 0.179                 | $0.08 \pm 0.07$      |
|                  | $\sigma^2 = 7\%$  | 1.00                | $1.04 \pm 0.22$       | $0.28 \pm 0.10$       | 0.196                 | $0.05 \pm 0.08$      |
|                  | $\sigma^2 = 10\%$ | 1.00                | $1.03 \pm 0.17$       | $0.31 \pm 0.18$       | 0.239                 | $0.02 \pm 0.05$      |
|                  | $u = 0.05$        | 1.00                | $1.02 \pm 0.14$       | $0.16 \pm 0.06$       | 0.120                 | $0.11 \pm 0.09$      |
|                  | $u = 0.10$        | 1.00                | $1.01 \pm 0.10$       | $0.16 \pm 0.06$       | 0.113                 | $0.11 \pm 0.10$      |
| COMPAS           | $\sigma^2 = 3\%$  | 1.00                | $1.00 \pm 0.00$       | $0.04 \pm 0.02$       | 0.417                 | $0.03 \pm 0.08$      |
|                  | $\sigma^2 = 7\%$  | 1.00                | $1.00 \pm 0.00$       | $0.04 \pm 0.02$       | 0.437                 | $0.01 \pm 0.03$      |
|                  | $\sigma^2 = 10\%$ | 1.00                | $1.00 \pm 0.00$       | $0.04 \pm 0.04$       | 0.452                 | $0.01 \pm 0.01$      |
|                  | $u = 0.05$        | 1.00                | $1.00 \pm 0.00$       | $0.04 \pm 0.02$       | 0.424                 | $0.04 \pm 0.01$      |
|                  | $u = 0.10$        | 1.00                | $1.00 \pm 0.00$       | $0.04 \pm 0.02$       | 0.410                 | $0.05 \pm 0.02$      |

only experiment with  $\tau$  up to 0.9, as setting  $\tau$  greater than 0.9 would further sacrifice efficacy. Our results also support the argument by Pawelczyk et al. [2023] that there is a trade-off between cost ( $\ell_1$  distance) and robustness to one-off noise.

### B.1.2 Accumulated Plausible Noise

When ROSE-mul generates recourse that is robust to the accumulated plausible noise, the hyper-parameters that would influence its robustness are  $\sigma^2$ ,  $u$  and  $\tau$ . In ROSE-mul,  $\sigma^2$  is the percentage of the size of one-off noise, which is added to each action unit  $u$ . Table B1 shows the performance of ROSE-mul under different  $\sigma^2$  and  $u$ . A bigger  $\sigma^2$  indicates that, when generating recourse, each action unit is robustified against bigger noise. A bigger  $u$  means that fewer actions are involved in the recourse, thus noise is added less frequently. All of the recourse generated under different hyper-parameters are evaluated with the same scale of noise perturbation. In general, as Acc AIR decreases,  $\ell_1$  distance of recourse increases. In other words, a higher level of robustness comes at a cost of longer recourse. More robust recourse also requires more computation time. Further, in the German Credit dataset, achieving higher robustness also sacrifices the efficacy of our method.  $\tau$  has the same effect on ROSE-one and ROSE-mul.

**Table B2:** Different  $\sigma^2$  in one-off plausible noise during evaluation. The configurations of all methods remain the same as the set-ups described in Section 5.1 and Table 1. In this table, we further report Plausible AIR of all methods under  $\sigma^2 = \{0.015, 0.01, 0.005\}$ .

|               |          | Plausible AIR                     |                                   |                                   |
|---------------|----------|-----------------------------------|-----------------------------------|-----------------------------------|
| Approach      |          | $\sigma^2 = 0.005$                | $\sigma^2 = 0.01$                 | $\sigma^2 = 0.015$                |
| German Credit | Wachter  | 0.56 $\pm$ 0.11                   | 0.79 $\pm$ 0.16                   | 0.80 $\pm$ 0.11                   |
|               | GrSp     | 0.52 $\pm$ 0.11                   | 0.77 $\pm$ 0.15                   | 0.78 $\pm$ 0.11                   |
|               | DiCE     | 0.21 $\pm$ 0.21                   | 0.26 $\pm$ 0.22                   | 0.32 $\pm$ 0.23                   |
|               | FASTAR   | 0.52 $\pm$ 0.10                   | 0.54 $\pm$ 0.11                   | 0.55 $\pm$ 0.11                   |
|               | CoGS     | 0.38 $\pm$ 0.09                   | 0.44 $\pm$ 0.11                   | 0.47 $\pm$ 0.11                   |
|               | PROBE    | 0.47 $\pm$ 0.04                   | 0.66 $\pm$ 0.18                   | 0.68 $\pm$ 0.10                   |
|               | CROCO    | 0.15 $\pm$ 0.14                   | 0.16 $\pm$ 0.13                   | 0.25 $\pm$ 0.11                   |
|               | ROSE-one | 0.13 $\pm$ 0.19                   | 0.22 $\pm$ 0.09                   | 0.28 $\pm$ 0.08                   |
|               | ROSE-mul | <b>0.09 <math>\pm</math> 0.09</b> | <b>0.10 <math>\pm</math> 0.04</b> | <b>0.23 <math>\pm</math> 0.08</b> |
| Adult Income  | Wachter  | 0.73 $\pm$ 0.14                   | 0.75 $\pm$ 0.15                   | 0.76 $\pm$ 0.15                   |
|               | GrSp     | 0.65 $\pm$ 0.15                   | 0.68 $\pm$ 0.16                   | 0.69 $\pm$ 0.16                   |
|               | DiCE     | 0.19 $\pm$ 0.26                   | 0.36 $\pm$ 0.30                   | 0.37 $\pm$ 0.21                   |
|               | FASTAR   | 0.68 $\pm$ 0.15                   | 0.75 $\pm$ 0.14                   | 0.77 $\pm$ 0.14                   |
|               | CoGS     | 0.70 $\pm$ 0.18                   | 0.76 $\pm$ 0.17                   | 0.77 $\pm$ 0.16                   |
|               | PROBE    | 0.30 $\pm$ 0.37                   | 0.37 $\pm$ 0.40                   | 0.36 $\pm$ 0.40                   |
|               | CROCO    | 0.38 $\pm$ 0.16                   | 0.54 $\pm$ 0.28                   | 0.55 $\pm$ 0.18                   |
|               | ROSE-one | <b>0.05 <math>\pm</math> 0.03</b> | <b>0.19 <math>\pm</math> 0.07</b> | <b>0.30 <math>\pm</math> 0.09</b> |
|               | ROSE-mul | 0.06 $\pm$ 0.05                   | 0.26 $\pm$ 0.10                   | 0.31 $\pm$ 0.12                   |
| COMPAS        | Wachter  | 0.48 $\pm$ 0.18                   | 0.79 $\pm$ 0.10                   | 0.80 $\pm$ 0.18                   |
|               | GrSp     | 0.48 $\pm$ 0.19                   | 0.75 $\pm$ 0.10                   | 0.76 $\pm$ 0.06                   |
|               | DiCE     | 0.10 $\pm$ 0.13                   | 0.21 $\pm$ 0.16                   | 0.24 $\pm$ 0.18                   |
|               | FASTAR   | 0.09 $\pm$ 0.12                   | 0.15 $\pm$ 0.14                   | 0.18 $\pm$ 0.13                   |
|               | CoGS     | 0.23 $\pm$ 0.12                   | 0.29 $\pm$ 0.15                   | 0.30 $\pm$ 0.14                   |
|               | PROBE    | 0.51 $\pm$ 0.16                   | 0.73 $\pm$ 0.11                   | 0.73 $\pm$ 0.17                   |
|               | CROCO    | 0.06 $\pm$ 0.05                   | 0.12 $\pm$ 0.12                   | 0.17 $\pm$ 0.10                   |
|               | ROSE-one | <b>0.04 <math>\pm</math> 0.05</b> | <b>0.11 <math>\pm</math> 0.08</b> | <b>0.15 <math>\pm</math> 0.09</b> |
|               | ROSE-mul | 0.05 $\pm$ 0.05                   | <b>0.11 <math>\pm</math> 0.08</b> | 0.16 $\pm$ 0.09                   |

**Table B3:** Different  $\sigma^2$  in accumulated plausible noise with fixed action size unit  $u = 0.025$ . The configurations of all methods remain the same as the set-ups described in Section 5.1 and Table 1, therefore only Acc AIR differs under different  $\sigma^2$  in accumulated plausible noise. In Table 1, 5% of the size of the one-off noise ( $\sigma^2 = 0.0005$ ) was added to each action unit. In this table, we further report Acc AIR of all methods under  $\sigma^2 = \{3\%(0.0003), 5\%(0.0005), 7\%(0.0007), 10\%(0.001)\}$  of the size of one-off noise.

|               |          | Acc AIR            |                    |                    |                    |
|---------------|----------|--------------------|--------------------|--------------------|--------------------|
| Approach      |          | $\sigma^2 = 3\%$   | $\sigma^2 = 5\%$   | $\sigma^2 = 7\%$   | $\sigma^2 = 10\%$  |
| German Credit | Wachter  | 0.55 ± 0.10        | 0.75 ± 0.17        | 0.77 ± 0.12        | 0.78 ± 0.11        |
|               | GrSp     | 0.56 ± 0.13        | 0.77 ± 0.18        | 0.78 ± 0.15        | 0.79 ± 0.13        |
|               | DiCE     | 0.27 ± 0.21        | 0.32 ± 0.20        | 0.34 ± 0.21        | 0.36 ± 0.19        |
|               | FASTAR   | 0.49 ± 0.14        | 0.51 ± 0.14        | 0.52 ± 0.14        | 0.52 ± 0.13        |
|               | CoGS     | 0.37 ± 0.12        | 0.41 ± 0.14        | 0.41 ± 0.11        | 0.44 ± 0.12        |
|               | PROBE    | 0.41 ± 0.16        | 0.70 ± 0.27        | 0.73 ± 0.18        | 0.74 ± 0.16        |
|               | CROCO    | 0.23 ± 0.12        | 0.25 ± 0.13        | 0.35 ± 0.07        | 0.38 ± 0.05        |
|               | ROSE-one | 0.21 ± 0.14        | 0.28 ± 0.05        | 0.31 ± 0.15        | 0.34 ± 0.14        |
|               | ROSE-mul | <b>0.20 ± 0.04</b> | <b>0.23 ± 0.02</b> | <b>0.29 ± 0.19</b> | <b>0.33 ± 0.18</b> |
| Adult Income  | Wachter  | 0.65 ± 0.17        | 0.68 ± 0.18        | 0.71 ± 0.18        | 0.72 ± 0.19        |
|               | GrSp     | 0.54 ± 0.17        | 0.60 ± 0.17        | 0.62 ± 0.17        | 0.65 ± 0.16        |
|               | DiCE     | 0.30 ± 0.22        | 0.45 ± 0.24        | 0.48 ± 0.25        | 0.48 ± 0.32        |
|               | FASTAR   | 0.42 ± 0.16        | 0.51 ± 0.18        | 0.55 ± 0.17        | 0.59 ± 0.17        |
|               | CoGS     | 0.46 ± 0.27        | 0.56 ± 0.27        | 0.61 ± 0.25        | 0.65 ± 0.24        |
|               | PROBE    | 0.45 ± 0.17        | 0.47 ± 0.18        | 0.49 ± 0.16        | 0.51 ± 0.16        |
|               | CROCO    | 0.21 ± 0.12        | 0.26 ± 0.25        | 0.29 ± 0.07        | 0.30 ± 0.18        |
|               | ROSE-one | 0.04 ± 0.07        | 0.11 ± 0.11        | 0.19 ± 0.15        | 0.28 ± 0.17        |
|               | ROSE-mul | <b>0.01 ± 0.04</b> | <b>0.04 ± 0.06</b> | <b>0.09 ± 0.10</b> | <b>0.14 ± 0.10</b> |
| COMPAS        | Wachter  | 0.47 ± 0.16        | 0.67 ± 0.16        | 0.67 ± 0.23        | 0.69 ± 0.12        |
|               | GrSp     | 0.45 ± 0.13        | 0.50 ± 0.16        | 0.53 ± 0.17        | 0.54 ± 0.22        |
|               | DiCE     | 0.19 ± 0.12        | 0.31 ± 0.13        | 0.34 ± 0.14        | 0.35 ± 0.13        |
|               | FASTAR   | 0.03 ± 0.01        | 0.05 ± 0.16        | 0.05 ± 0.11        | 0.05 ± 0.11        |
|               | CoGS     | 0.15 ± 0.14        | 0.22 ± 0.15        | 0.24 ± 0.14        | 0.28 ± 0.15        |
|               | PROBE    | 0.29 ± 0.13        | 0.65 ± 0.16        | 0.68 ± 0.17        | 0.69 ± 0.15        |
|               | CROCO    | 0.04 ± 0.05        | 0.05 ± 0.07        | 0.06 ± 0.04        | 0.08 ± 0.03        |
|               | ROSE-one | <b>0.01 ± 0.02</b> | <b>0.01 ± 0.03</b> | <b>0.02 ± 0.04</b> | <b>0.02 ± 0.05</b> |
|               | ROSE-mul | <b>0.01 ± 0.04</b> | <b>0.01 ± 0.03</b> | <b>0.02 ± 0.04</b> | <b>0.02 ± 0.04</b> |

**Table B4:** Different action unit size  $u$  in accumulated plausible noise;  $\sigma^2$  is fixed to  $\sigma^2 = 0.0005$ .

|               |              | $u = 0.025$         |                                   | $u = 0.05$          |                                   | $u = 0.10$         |                                   |
|---------------|--------------|---------------------|-----------------------------------|---------------------|-----------------------------------|--------------------|-----------------------------------|
| Approach      |              | # of steps          | Acc AIR                           | # of steps          | Acc AIR                           | # of steps         | Acc AIR                           |
| German Credit | Wachter      | 18.55 $\pm$ 12.16   | 0.75 $\pm$ 0.17                   | 9.27 $\pm$ 6.08     | 0.54 $\pm$ 0.12                   | 4.64 $\pm$ 3.04    | 0.51 $\pm$ 0.11                   |
|               | GrSp         | 43.92 $\pm$ 31.19   | 0.77 $\pm$ 0.18                   | 21.96 $\pm$ 15.59   | 0.55 $\pm$ 0.13                   | 10.98 $\pm$ 7.80   | 0.50 $\pm$ 0.12                   |
|               | DiCE         | 44.83 $\pm$ 16.78   | 0.32 $\pm$ 0.20                   | 22.41 $\pm$ 8.39    | 0.26 $\pm$ 0.20                   | 22.21 $\pm$ 4.19   | 0.20 $\pm$ 0.18                   |
|               | FASTAR       | 17.22 $\pm$ 13.61   | 0.51 $\pm$ 0.14                   | 8.61 $\pm$ 6.81     | 0.49 $\pm$ 0.14                   | 4.31 $\pm$ 3.43    | 0.45 $\pm$ 0.14                   |
|               | CoGS         | 19.95 $\pm$ 13.44   | 0.41 $\pm$ 0.14                   | 9.98 $\pm$ 6.72     | 0.34 $\pm$ 0.13                   | 4.98 $\pm$ 3.36    | 0.26 $\pm$ 0.14                   |
|               | PROBE        | 55.09 $\pm$ 31.91   | 0.70 $\pm$ 0.27                   | 27.55 $\pm$ 15.90   | 0.40 $\pm$ 0.18                   | 13.78 $\pm$ 7.95   | 0.26 $\pm$ 0.13                   |
|               | CROCO        | 49.21 $\pm$ 17.37   | 0.25 $\pm$ 0.13                   | 24.61 $\pm$ 8.69    | 0.23 $\pm$ 0.11                   | 12.31 $\pm$ 4.35   | 0.19 $\pm$ 0.16                   |
|               | ROSE-one     | 21.60 $\pm$ 13.21   | 0.28 $\pm$ 0.05                   | 10.84 $\pm$ 6.61    | 0.20 $\pm$ 0.13                   | 5.42 $\pm$ 3.31    | 0.12 $\pm$ 0.11                   |
|               | ROSE-mul     | 21.60 $\pm$ 12.80   | <b>0.23 <math>\pm</math> 0.02</b> | 10.82 $\pm$ 6.40    | <b>0.19 <math>\pm</math> 0.13</b> | 5.41 $\pm$ 3.21    | <b>0.10 <math>\pm</math> 0.11</b> |
|               | Adult Income | Wachter             | 11.48 $\pm$ 6.92                  | 0.68 $\pm$ 0.18     | 5.74 $\pm$ 3.46                   | 0.63 $\pm$ 0.17    | 2.87 $\pm$ 1.73                   |
| GrSp          |              | 28.15 $\pm$ 30.40   | 0.60 $\pm$ 0.17                   | 14.10 $\pm$ 15.20   | 0.53 $\pm$ 0.18                   | 7.04 $\pm$ 7.60    | 0.45 $\pm$ 0.20                   |
| DiCE          |              | 43.82 $\pm$ 20.40   | 0.45 $\pm$ 0.24                   | 21.91 $\pm$ 10.20   | 0.39 $\pm$ 0.21                   | 10.96 $\pm$ 5.10   | 0.25 $\pm$ 0.20                   |
| FASTAR        |              | 3.60 $\pm$ 2.01     | 0.51 $\pm$ 0.18                   | 1.82 $\pm$ 1.03     | 0.40 $\pm$ 0.18                   | 0.93 $\pm$ 0.54    | 0.28 $\pm$ 0.17                   |
| CoGS          |              | 4.61 $\pm$ 2.33     | 0.56 $\pm$ 0.27                   | 2.31 $\pm$ 1.16     | 0.43 $\pm$ 0.27                   | 1.15 $\pm$ 0.58    | 0.28 $\pm$ 0.24                   |
| PROBE         |              | 489.66 $\pm$ 265.49 | 0.47 $\pm$ 0.18                   | 244.83 $\pm$ 132.74 | 0.44 $\pm$ 0.19                   | 122.41 $\pm$ 66.37 | 0.40 $\pm$ 0.20                   |
| CROCO         |              | 9.59 $\pm$ 4.87     | 0.26 $\pm$ 0.25                   | 4.80 $\pm$ 0.44     | 0.18 $\pm$ 0.17                   | 2.41 $\pm$ 0.22    | 0.27 $\pm$ 0.13                   |
| ROSE-one      |              | 7.20 $\pm$ 2.40     | 0.11 $\pm$ 0.11                   | 3.60 $\pm$ 1.21     | 0.03 $\pm$ 0.06                   | 1.83 $\pm$ 0.63    | <b>0.00 <math>\pm</math> 0.01</b> |
| ROSE-mul      |              | 8.80 $\pm$ 4.80     | <b>0.04 <math>\pm</math> 0.06</b> | 4.42 $\pm$ 2.42     | <b>0.01 <math>\pm</math> 0.04</b> | 2.21 $\pm$ 1.21    | <b>0.00 <math>\pm</math> 0.00</b> |
| COMPAS        |              | Wachter             | 7.41 $\pm$ 5.89                   | 0.67 $\pm$ 0.16     | 3.70 $\pm$ 2.95                   | 0.47 $\pm$ 0.18    | 1.85 $\pm$ 1.47                   |
|               | GrSp         | 10.08 $\pm$ 11.93   | 0.50 $\pm$ 0.16                   | 5.04 $\pm$ 5.97     | 0.51 $\pm$ 0.16                   | 2.52 $\pm$ 2.98    | 0.51 $\pm$ 0.16                   |
|               | DiCE         | 33.76 $\pm$ 20.30   | 0.31 $\pm$ 0.13                   | 16.88 $\pm$ 10.15   | 0.26 $\pm$ 0.10                   | 8.44 $\pm$ 5.08    | 0.13 $\pm$ 0.10                   |
|               | FASTAR       | 1.20 $\pm$ 0.40     | 0.05 $\pm$ 0.11                   | 0.60 $\pm$ 0.20     | 0.03 $\pm$ 0.09                   | 0.30 $\pm$ 0.10    | 0.02 $\pm$ 0.08                   |
|               | CoGS         | 9.26 $\pm$ 4.84     | 0.22 $\pm$ 0.15                   | 4.63 $\pm$ 2.42     | 0.13 $\pm$ 0.13                   | 2.31 $\pm$ 1.21    | 0.05 $\pm$ 0.08                   |
|               | PROBE        | 21.17 $\pm$ 12.49   | 0.65 $\pm$ 0.16                   | 10.58 $\pm$ 6.24    | 0.45 $\pm$ 0.16                   | 5.29 $\pm$ 3.12    | 0.23 $\pm$ 0.15                   |
|               | CROCO        | 19.74 $\pm$ 8.63    | 0.05 $\pm$ 0.07                   | 9.87 $\pm$ 4.32     | 0.03 $\pm$ 0.05                   | 4.94 $\pm$ 2.16    | 0.03 $\pm$ 0.08                   |
|               | ROSE-one     | 1.60 $\pm$ 0.80     | <b>0.01 <math>\pm</math> 0.03</b> | 0.80 $\pm$ 0.40     | <b>0.01 <math>\pm</math> 0.02</b> | 0.40 $\pm$ 0.20    | <b>0.00 <math>\pm</math> 0.00</b> |
|               | ROSE-mul     | 1.60 $\pm$ 0.80     | <b>0.01 <math>\pm</math> 0.03</b> | 0.80 $\pm$ 0.40     | <b>0.01 <math>\pm</math> 0.02</b> | 0.40 $\pm$ 0.20    | 0.01 $\pm$ 0.05                   |

## B.2 Different Magnitude of Noise for Evaluation

### B.2.1 One-off Plausible Noise

In this section, we report the invalidation rates for different sizes of one-off plausible noise when evaluating all methods, and show the results in Table B2. For all methods across all datasets, as  $\sigma^2$  gets larger, the invalidation rate increases. ROSE-one or ROSE-mul maintains the lowest invalidation rate across all experiments.

### B.2.2 Accumulated Plausible Noise

In this section we report the performance of different methods in terms of different magnitudes of accumulated plausible noise. Both the unit size of an action –  $u$  – and the variance of noise added to each action unit –  $\sigma^2$  – influence the magnitude of accumulated noise used for evaluation. Table B3 and Table B4 report the performance by varying either  $\sigma^2$  or  $u$  and fixing the other. Across all datasets, Acc AIR of all methods increases as the value of  $\sigma^2$  increases (Table B3); Acc AIR decreases as the value of  $u$  increases (Table B4). ROSE-mul consistently outperforms other methods in terms of Acc AIR.

## B.3 Performance of Additional Baselines

In this section, we report the performance of two other baselines – ROAR and ARAR. ROAR is designed to be robust against model shifts [Upadhyay et al., 2021]. We explore whether ROAR is also robust to noisy human implementation of recourse. The other baseline, ARAR, is robust to noisy user inputs [Dominguez-Olmedo et al., 2022]. However, ARAR is only compatible with logistic regression classifiers; its efficacy is as low as 0.02 when the underlying classifier is a neural network [Pawelczyk et al., 2023]. Therefore, in Table B5, we report the performance of all baselines that are designed to produce recourse that is robust to varying adversarial events. For a fair comparison, and to showcase that ROSE is agnostic to different classifiers (i.e., model-agnostic), we use logistic regression for classification.

## B.4 Detailed Comparison with ROAR and ARAR

In this section, we further discuss the performance of ROAR and ARAR reported in Table B5. When the underlying classifier is a linear model, both ROAR and ARAR have good performance in finding valid recourse (i.e., efficacy is 100% or near 100%) in a short time. For ROAR, the invalidation rates of one-off noise and accumulated noise are zero or close to zero across all datasets. ARAR can maintain a low invalidation rate on the COMPAS and German Credit datasets. However, achieving high robustness comes at a cost of high  $\ell_1$  distance and high sparsity. Specifically, recourse produced by ARAR requests all users to change every single feature across all datasets; ROAR provides recourse that changes at least half of the feature set. In reality, high sparsity indicates high complexity and more effort, thus is less preferable.

In addition, ARAR provides recourse with up to 10 times higher  $\ell_1$  distance than our method ROSE. Distances of recourse by ROAR can be up to 30 times higher than that of ROSE. To visually understand the magnitude of such difference, we compare

**Table B5:** Comparing ROSE with two additional baselines, ROAR and ARAR, and three previously discussed baselines, CoGS, PROBE and CROCO. The underlying predictor is a logistic regression model. For ROAR, we set learning rate = 0.1; For ARAR, we set  $\epsilon = 0.01$ . The set-ups for the remaining methods are the same as the set-ups described in Table 1.

|        |          | Metrics             |                                   |                                   |                       |                                   |                                   |                                   |
|--------|----------|---------------------|-----------------------------------|-----------------------------------|-----------------------|-----------------------------------|-----------------------------------|-----------------------------------|
|        | Approach | Efficacy $\uparrow$ | Sparsity $\downarrow$             | $\ell_1$ $\downarrow$             | Time (s) $\downarrow$ | Gaussian AIR $\downarrow$         | Plausible AIR $\downarrow$        | Acc AIR $\downarrow$              |
| German | ROAR     | <b>1.00</b>         | 20.00 $\pm$ 0.00                  | 10.56 $\pm$ 1.95                  | <b>0.015</b>          | <b>0.00 <math>\pm</math> 0.00</b> | <b>0.00 <math>\pm</math> 0.00</b> | <b>0.00 <math>\pm</math> 0.00</b> |
|        | ARAR     | 0.99                | 20.00 $\pm$ 0.00                  | 3.83 $\pm$ 0.50                   | 0.086                 | <b>0.00 <math>\pm</math> 0.00</b> | <b>0.00 <math>\pm</math> 0.00</b> | 0.08 $\pm$ 0.08                   |
|        | CoGS     | <b>1.00</b>         | 6.94 $\pm$ 1.20                   | 0.36 $\pm$ 0.23                   | 1.622                 | 0.39 $\pm$ 0.04                   | 0.43 $\pm$ 0.07                   | 0.37 $\pm$ 0.11                   |
|        | PROBE    | <b>1.00</b>         | 20.00 $\pm$ 0.00                  | 1.16 $\pm$ 0.65                   | 1.271                 | 0.22 $\pm$ 0.03                   | 0.33 $\pm$ 0.06                   | 0.38 $\pm$ 0.13                   |
|        | CROCO    | 0.55                | 20.00 $\pm$ 0.00                  | 1.14 $\pm$ 0.40                   | 0.198                 | 0.11 $\pm$ 0.05                   | 0.11 $\pm$ 0.12                   | 0.17 $\pm$ 0.08                   |
|        | ROSE-one | 0.65                | <b>1.53 <math>\pm</math> 0.79</b> | 0.33 $\pm$ 0.35                   | 0.086                 | 0.10 $\pm$ 0.06                   | 0.11 $\pm$ 0.07                   | 0.14 $\pm$ 0.14                   |
|        | ROSE-mul | 0.65                | <b>1.53 <math>\pm</math> 0.79</b> | <b>0.32 <math>\pm</math> 0.33</b> | 0.152                 | 0.09 $\pm$ 0.04                   | 0.08 $\pm$ 0.06                   | 0.19 $\pm$ 0.25                   |
| Adult  | ROAR     | <b>1.00</b>         | 6.00 $\pm$ 0.00                   | 3.09 $\pm$ 0.72                   | 0.041                 | <b>0.00 <math>\pm</math> 0.00</b> | <b>0.00 <math>\pm</math> 0.00</b> | 0.06 $\pm$ 0.08                   |
|        | ARAR     | <b>1.00</b>         | 13.00 $\pm$ 0.00                  | 2.56 $\pm$ 0.78                   | 0.194                 | 0.03 $\pm$ 0.01                   | 0.30 $\pm$ 0.28                   | 0.53 $\pm$ 0.28                   |
|        | CoGS     | <b>1.00</b>         | 4.90 $\pm$ 0.33                   | 0.35 $\pm$ 0.19                   | 3.864                 | 0.38 $\pm$ 0.12                   | 0.79 $\pm$ 0.24                   | 0.67 $\pm$ 0.24                   |
|        | PROBE    | <b>1.00</b>         | 13.00 $\pm$ 0.00                  | 1.64 $\pm$ 1.18                   | 2.731                 | 0.31 $\pm$ 0.04                   | 0.76 $\pm$ 0.19                   | 0.75 $\pm$ 0.21                   |
|        | CROCO    | 0.98                | 6.00 $\pm$ 0.00                   | 0.43 $\pm$ 0.07                   | 0.634                 | 0.08 $\pm$ 0.05                   | 0.23 $\pm$ 0.08                   | 0.24 $\pm$ 0.13                   |
|        | ROSE-one | <b>1.00</b>         | <b>1.01 <math>\pm</math> 0.10</b> | <b>0.17 <math>\pm</math> 0.04</b> | <b>0.030</b>          | 0.05 $\pm$ 0.02                   | 0.17 $\pm$ 0.06                   | 0.09 $\pm$ 0.08                   |
|        | ROSE-mul | <b>1.00</b>         | 1.04 $\pm$ 0.20                   | 0.23 $\pm$ 0.10                   | 0.186                 | 0.05 $\pm$ 0.02                   | 0.19 $\pm$ 0.08                   | <b>0.02 <math>\pm</math> 0.03</b> |
| COMPAS | ROAR     | <b>1.00</b>         | 4.00 $\pm$ 4.00                   | 1.67 $\pm$ 0.23                   | <b>0.015</b>          | <b>0.00 <math>\pm</math> 0.00</b> | <b>0.00 <math>\pm</math> 0.00</b> | <b>0.00 <math>\pm</math> 0.01</b> |
|        | ARAR     | <b>1.00</b>         | 7.00 $\pm$ 0.00                   | 1.07 $\pm$ 0.28                   | 0.072                 | 0.03 $\pm$ 0.01                   | 0.07 $\pm$ 0.08                   | 0.08 $\pm$ 0.09                   |
|        | CoGS     | <b>1.00</b>         | 2.88 $\pm$ 0.32                   | <b>0.25 <math>\pm</math> 0.14</b> | 1.279                 | 0.26 $\pm$ 0.02                   | 0.27 $\pm$ 0.12                   | 0.19 $\pm$ 0.13                   |
|        | PROBE    | <b>1.00</b>         | 7.00 $\pm$ 0.00                   | 0.61 $\pm$ 0.36                   | 1.231                 | 0.34 $\pm$ 0.02                   | 0.32 $\pm$ 0.16                   | 0.27 $\pm$ 0.15                   |
|        | CROCO    | <b>1.00</b>         | 5.00 $\pm$ 0.00                   | 0.54 $\pm$ 0.17                   | 0.118                 | 0.13 $\pm$ 0.02                   | 0.25 $\pm$ 0.17                   | 0.26 $\pm$ 0.11                   |
|        | ROSE-one | <b>1.00</b>         | <b>1.00 <math>\pm</math> 0.00</b> | 0.30 $\pm$ 0.05                   | 0.156                 | 0.11 $\pm$ 0.07                   | 0.21 $\pm$ 0.05                   | 0.24 $\pm$ 0.09                   |
|        | ROSE-mul | <b>1.00</b>         | <b>1.00 <math>\pm</math> 0.00</b> | 0.48 $\pm$ 0.13                   | 3.113                 | 0.09 $\pm$ 0.04                   | 0.21 $\pm$ 0.05                   | 0.05 $\pm$ 0.10                   |



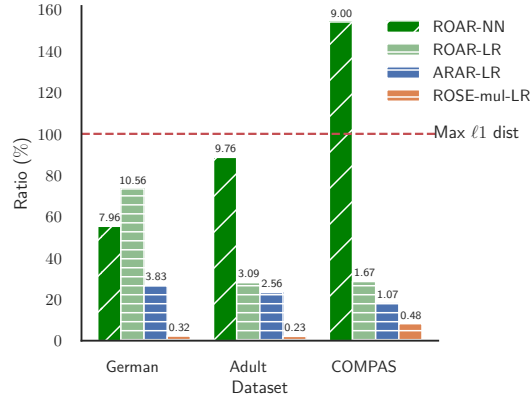


**Fig. B3:** Comparisons of recourse by different robust methods in terms of  $\ell_1$  distance. We report the results of ROAR under both a neural network (NN) and a logistic regression (LR) classifier. ARAR does not support NN, so we omit its corresponding result. The distances of recourse by ROSE-one and ROSE-mul under LR and NN are similar, thus we only report one result in this figure. The red dotted line indicates the distance between two further points in each dataset, and the y-axis indicates the ratio of the average recourse distance to the maximum data-points distance. The actual  $\ell_1$  distance of recourse is annotated on the top of each bar.

the average distance of recourse provided by ROAR, ARAR and ROSE against the maximum  $\ell_1$  distance between the two furthest data points in a dataset. As shown in Figure B3, under a logistic regression classifier,  $\ell_1$  distances in ROAR and ARAR are notably higher than ROSE-mul. We further find out that, if a neural network is used as the classifier, the average distance of recourse by ROAR can be even longer than the distance between two furthest data points in a dataset. This implies that, if users follow recourse by ROAR, they have to move across all data points. In summary, even though ROAR and ARAR are robust to noisy human implementation, their recourse is impractical for users to follow.

It is also worth noting that ARAR is only compatible with linear classifiers. Under non-linear classifiers, its efficacy is as low as 1-2% in each dataset. ROAR supports non-linear classifiers, although under such cases the distance of recourse increases. On the other hand, our method ROSE is model-agnostic, and the performance does not vary significantly across classifiers.

## Appendix C Implementation Details

### C.1 Datasets

Across all datasets, we use all features for classifier training as well as for recourse generation. We acknowledge that some features might be immutable – e.g., race – and some might be mutable but not actionable – e.g., age; some actionable features

could have also actionability constraints. However, the main focus of this work is on robustness. Following the practice in [Pawelczyk et al., 2023], we treat all features as actionable. Future work could be extended to address robustness and actionability simultaneously.

## C.2 Details about Classifiers

In Section 5.2, we use the neural network as the underlying classifier to determine the negative instances across all three datasets. Specifically, the neural network is fully connected, with ReLU activation function and a hidden layer of 50 neurons. Further, we use logistic regression as the underlying classifier across all datasets, for experiments presented in Appendix B.3. The training details are shown in Table C6. The performance of classifiers and the number of negative instances for which the recourse is generated are reported in Table C7.

**Table C6:** Training details for two classifiers on three datasets.

|               |    | German | Adult | COMPAS |
|---------------|----|--------|-------|--------|
| Batch size    | LR | 50     | 512   | 50     |
|               | NN | 512    | 512   | 512    |
| Epochs        | LR | 50     | 50    | 50     |
|               | NN | 50     | 50    | 50     |
| Learning rate | LR | 0.001  | 0.001 | 0.001  |
|               | NN | 0.002  | 0.002 | 0.002  |

**Table C7:** The first two rows show the accuracy of underlying classifiers. The last two rows show the number of negative instances (# of points) for which the recourse is generated.

|             |    | German | Adult | COMPAS |
|-------------|----|--------|-------|--------|
| Accuracy    | LR | 0.78   | 0.84  | 0.86   |
|             | NN | 0.83   | 0.85  | 0.86   |
| # of points | LR | 157    | 200   | 97     |
|             | NN | 285    | 200   | 104    |

## C.3 Implementation Details of Policy Gradient Method in ROSE

In this section, we provide more details about the policy-gradient method discussed in Section 4, which we use to solve our MDP problem. We use the off-the-shelf

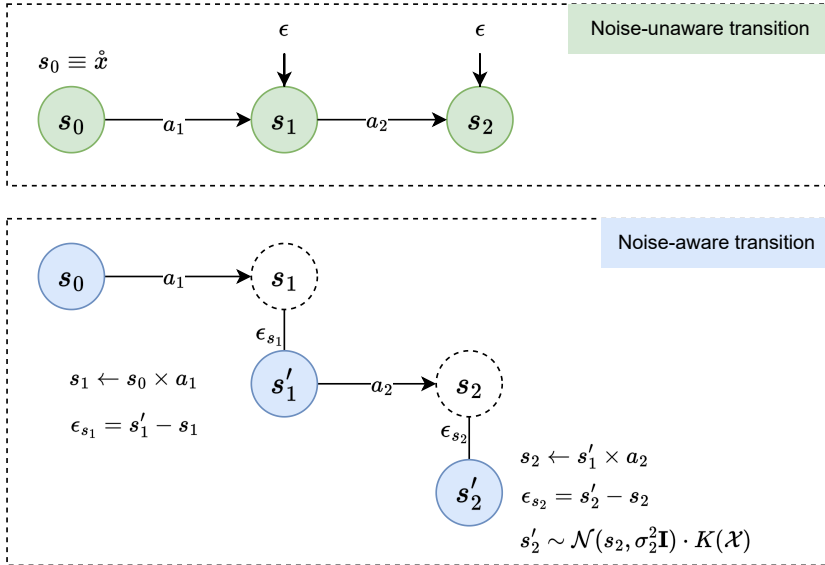


**Fig. C4:** Illustration of different noise that accumulates along the recourse with two actions  $a_1, a_2$ . The green path shows a noise-unaware transition after an action and white Gaussian noise (i.e.  $\epsilon \sim \mathcal{N}(0, \sigma^2 \cdot \mathbf{I})$ ) added to each state. The blue path shows a noise-aware transition where the subsequent action applies to the noisy state  $s'$ .

implementation of the PPO with GAE algorithm [Kostrikov, 2018]. To leverage this implementation of the PPO algorithm, we need to create the environment using the open-source toolkit OpenAI Gym library [Brockman et al., 2016]. The environment is created separately to model each dataset. In the PPO algorithm, both an actor and critic are approximated by neural networks – in our method, we use a fully connected neural network with two hidden layers and each layer having 64 neurons. For other hyper-parameters in the PPO algorithm, we follow the hyper-parameter set-up used in [Verma et al., 2022]. For training the PPO algorithm, we also follow their practice by using random data instances from the training set as the starting point – it is argued that this leads to better learning by the RL agent [Verma et al., 2022].

With the MDP set-up described in Section 4, the total rewards gained while training the PPO algorithm to learn the approximated policy converge fast. For ROSE-one, the one-time training cost for learning policies was 30 minutes for each of the three datasets. For ROSE-mul, the training time was about one hour for each dataset. We use the same CPU machine for training. Since the most time-consuming computation is calculating the IR of the accumulated plausible noise, using GPU does not accelerate the computation.

## Appendix D Proofs

### D.1 Proposition 2

**Proposition 2** (Accumulated Noise). *Assuming that noise can arise during the implementation of every recourse step, this noise would accumulate proportionally to the number of features changed and their magnitude required by every such step.*

**Proof** Eq. (5) shows that  $\epsilon_{s_i}$  is sampled based on the distribution  $s'_i \sim \mathcal{N}(s_i, \sigma_i^2 \mathbf{I}) \cdot K(\mathcal{X})$ , thus the size of  $\epsilon_{s_i}$  is proportional to  $\sigma_i^2$ . Given that  $\sigma_i^2 = \frac{\|a_i\|}{u} \times \sigma^2$ , this indicates that  $\epsilon_{s_i} \propto \|a_i\|$  where  $\|a_i\|$  is the magnitude of feature changes brought by each action. In addition, according to its definition, the accumulated noise is the sum of plausible noise added to each action unit. Namely,  $\mathcal{N}_{(\tilde{x}, \mathcal{A})}(\tilde{x}) \sim \sum_{i=1}^k \epsilon_{s_i}$  where  $k$  is the number of actions (i.e., the number of features changed) in the recourse. Thus we can conclude that the magnitude of accumulated plausible noise is proportional to the number of features changed and the magnitude of each feature change.  $\square$

### D.2 Proposition 3

**Proposition 3** (Markov Property of Noisy State Transition). *If the noise associated with each recourse action follows the plausible noise distribution, the distribution of the accumulated plausible noise depends upon the order and scale of said actions. Given the present  $s'_{i-1}$  and  $a_i$ , the subsequent  $\epsilon_{s_i}$  and  $s'_i$  do not depend on the past. In this case the noisy transition for  $s'_{i-1} \times a_i$  to  $s'_i$  satisfies the Markov property.*

**Proof** From Definition 2, we can read that  $s'_i$  is influenced and is only influenced by  $s'_{i-1}$  and  $a_i$ . Once  $s'_{i-1}$  and  $a_i$  are known, the distribution of  $s'_i$  is *conditionally independent* of all the previous actions  $a_{1, \dots, i-1}$  and intermediate states  $s'_{1, \dots, i-2}$ . Therefore the noisy transition from one state to the next satisfies the Markov property.

In Fig. C4 we also provide pictorial examples of modelling noisy implementation of recourse with (state-dependent) uniform noise and plausible noise that satisfies Markov property. When we add uniform noise to each action, we can simply ignore the noisy transition between states and sum up all  $\epsilon$  added to every state as the accumulated noise. On the other hand, when we consider plausible noise of which the distribution depends on the current state, we need to model the historical state transitions to determine the current state. Since  $s'_2$  is only dependent upon  $s'_1$  and  $a_2$ , and once fixing these two terms, previous state  $s_0$  and previous action  $a_1$  do not influence  $s'_2$ , therefore we can observe the Markov property in the distribution of plausible noise accumulated along recourse.  $\square$